Section 5

Development of and studies with regional and smaller-scale atmospheric models, regional ensemble forecasting

Adaptation of the PSU/NCAR MM5 for high-resolution weather prediction over Russia

L.V. Berkovich [1] , K.G. Rubinstein [1] , R.Ju. Ignatov [1] , G.M. Kalugina [2] , S.O. Krichak [3] , M.V. Tsidulko [3] , I.E. Zacharov [4]

[1] Hydrometeorological Research Center of Russia, Moscow,Russia,

[2] Hydrometeorological Bureau of Moscow and Moscow Region, Moscow, Russia,

[3] Tel Aviv University, Tel Aviv, Israel

[4] Silicon Graphics Inc.

E-mails: berkovich@mecom.ru, rubin@mecom.ru, ignatovroman@mail.ru, hmbkgu@hydromet.ru, shimon@cyclone.tau.ac.il, marina@cyclone.tau.ac.il, zacharov@sgi.com

The Penn State/NCAR mesoscale model MM5v3.6 has been adapted for high-resolution numerical weather prediction and computer benchmarking at the Main Computer Center (MCC) of the Hydrometeorological Service of Russia (Roshydromet). Initial and lateral boundary conditions for the developed system are being specified from the synoptic-scale numerical three-dimensional analyses and predictions available from the Hydrometcentre of Russia (HMC) and the National Center for Environmental Prediction (NCEP), USA. An automatic weather prediction system has been designed to allow realization of the all standard stages of the data processing and weather prediction with the MM5 both on the distributed memory and the distributed shared memory computers. No objective analysis computations are performed. Efficiency of the developed MM5-based system has been tested on the Itanium 2 Altix 3700, Origin 2000 Silicon Graphics and Xeon-2 computers. Three model versions (Table 1, I-III) have been configured with the aim of the experimental 72-hr weather prediction over Europe and Central part of European Russia (centered over Moscow). An example of a pattern with the results of the T850/H850 72 hr prediction initiated at 00:00 UTC June 4, 2004 is given in Figure 1. Results of the MM5 benchmarking on the Altix 3700 machine are presented in Table 2.

Future plans of work include detailed evaluation of the accuracy of the model predictions and the determination of its optimal configuration for the weather prediction over Russia.

Partial support has been provided by RFFI grants 03-05-64312, 04-05-64151 and INTAS project 03 -51- 5296.

Table 1. Configuration of the MM5 model versions at the HMC/MCC Russia

Experimental Version	I (Altix/Origin)	II (Xeon4)	III (Altix)
Num of levels	37	27	37
Num domains	4	2	27
Horiz. Res.	45/15/5/1 km	54/18 km	1x90/3x30/21x10km
Pressure at model top	70 hPa	70 hPa	70 km
Domain interaction	One-way	One-way	One-way
Init./boundary data	NCEP, USA	HMC, Russia	NCEP, USA
FDDA	No	No	No
Expl. Moisture	Simple ice	Simple ice	Simple ice
Cumulus scheme	G/G/0/0 (G=Grell)	G/G (B-M=Betts-Miller	B-M/K-F/G (K-F=Kain-Fritch)
Shallow conv.	No	No	No

PBL scheme	Eta M-Y	MRF	Eta M-Y
Radiation	RRTM	Cloud	RRTM
Land surface	NOAH	Multi-layer Soil temp.	NOAH
Effects of monthly snow albedo	Yes	No	Yes

Table 1 (cont)

Table 2. Benchmark estimations for 48-hr prediction with the MM5 (version III, Tabl. 1) on the SGI Altix 3700 (1.5 GHz/ 6.MB processors)

N.domains/resolution	N. grid points	N. of processors	Time (min)
1 (90 km)	85x100 points	16 processors	6 min
1 (30 km)	148x121	28	5 min 48 s
1 (30 km)	103x73	16	5 min 55 s
1 (30 km)	124x73	16	5 min 21 s
21 (10 km)	52 x 52	6	18 min x 21
21 (10 km)	52 x 52	60	3 min x 21

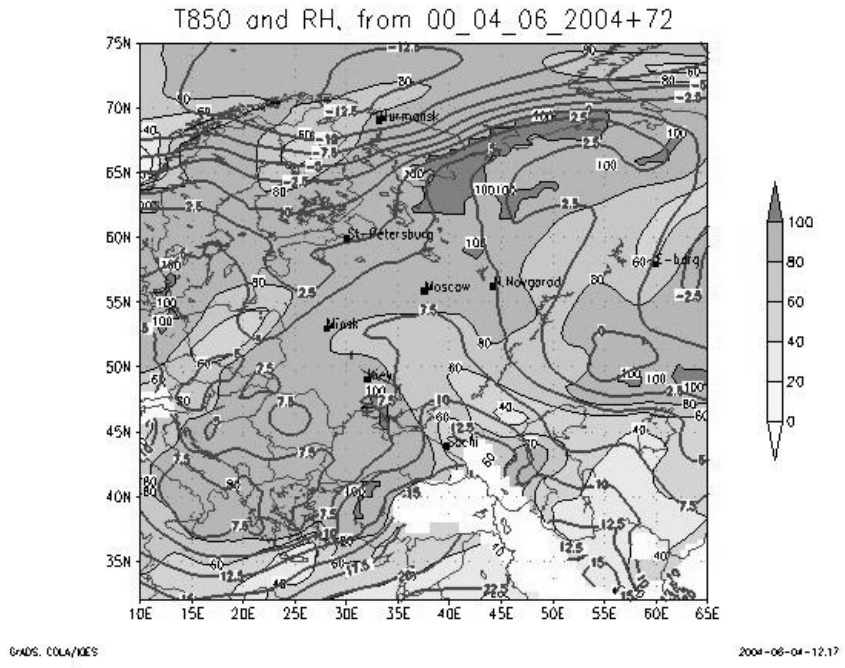

Figure 1: 72-hr forecast of the air temperature and relative humidity at 850 hPa

PRELIMINARY COMPARISON OF AMSR-E OBSERVATION AND NUMERICAL SIMULATION WITH CLOUD RESOLVING MODEL FOR SOLID PRECIPITATION IN WINTER DURING THE WAKASA 2003

Hisaki Eito[1], Kazumasa Aonashi[1], Guosheng Liu[2], Chiashi Muroi[1],
Syugo Hayashi[1], Teruyuki Kato[1], and Masanori Yoshizaki[1]

[1]*Meteorological Research Institute, Japan Meteorological Agency, Tsukuba, Ibaraki, 305-0052, Japan*
[2]*Florida State University, Tallahassee, FL 32306-4520, U.S.A.*

1. INTRODUCTION

For improving the accuracy of passive microwave solid precipitation retrieval algorithm using the AMSR/AMSR-E, the feild campaign (WAKASA2003) was conducted in the Fukui area, Japan, from January 12 to February 5, 2003. During the WAKASA2003, many active convective snowfall clouds frequently formed over the Sea of Japan due to cold outbreak. On 28-29 January 2003, broad cloud bands extending southeastward from the base of the Korean Peninsula to the Fukui area formed, and developed under the influence of the upper cold low. In this paper, high-resolution numerical simulations of these cloud bands are performed using a CRM with 1 km horizontal resolution. The expected brightness temperatures simulated by microwave radiative transfer model (MRTM) with CRM-derived atmospheric conditions were compared with AMSR-E observations. Our purposes are to check and improve the cloud microphysics scheme of the CRM, and to supply useful information from the model-derived 3-D structures of precipitation for improving the accuracy of the AMSR-E precipitation retrieval algorithm.

2. OBSERVATIONS

Figure 1 shows the GMS-5 visible imagery at 13 JST on 29 January 2003. Several clouds were found over the Sea of Japan, as a consequence of heat and moisture supply to continental cold air mass. The remarkable cloud bands, where cumulus convections developed, were distributed over the Sea of Japan from the base of the Korean Peninsula to the Tohoku district of Japan. It is well known that these cloud bands form over the low-level convergence zone (Japan Sea Polar-air mass Convergence Zone; JPCZ) between two cold airflows with different property (Nagata et al., 1986; Nagata, 1991; Nagata, 1992). These cloud bands formed in the previous day (28 Jan.), and developed under the influence of upper cold low (Fig. 1).

In this time, there are observations of AMSR-E, which is a microwave radiometer aboard AQUA satellite. Figure 2 is the scattering index retrieved from 89 GHz britness temperature of AMSR-E. Colors varying from black to white correspond to increasing scattering. The areas with large scattering index, where a amount of snow and graupel perticles is large, were distributed over the Sea of Japan. These areas well corresponded to high radar reflectivity intensity areas observed by JMA operational radar(not shown).

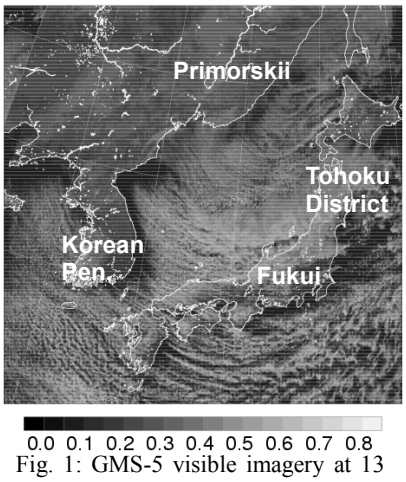

Fig. 1: GMS-5 visible imagery at 13 JST on 29 January 2003.

3. NUMERICAL MODELS

The CRM developed by Japan Meteorological Agency (JMA) is used in this study (JMA-NHM: Saito et al., 2001). The fully compressible equations with the conformal mapping are employed as the basic equations of the JMA-NHM. Primary physical processes such as cloud physics, atmospheric radiation and mixing in the planetary boundary layer are also included in the JMA-NHM. The bulk cloud microphysics scheme is employed in the JMA-NHM. This scheme predicts the mixing ratios of six water species (water vapor, cloud water, rain, cloud ice, snow and graupel) and the number concentrations of five condensed water species. The JMA-NHM has been transferred to the Earth Simulator (ES), which is the fastest supercomputer in the world. In the present study, the JMA-NHM has a horizontal grid size of 1km with 2000 x 2000 grid points. The vertical grid with a terrain-following coordinate contains 38 levels with a variable grid interval of 40 m near the surface and 1090 m at the top of the domain. The model top is 20.36 km. The time step interval is 5 seconds. The initial and boundary conditions for the JMA-NHM are provided from output produced by Regional Spectral Model (RSM). The RSM with a horizontal grid size of about 20km is a hydrostatic model used operationally in JMA. Radiative transfer calculations are performed with a 4 stream MRTM (Liu, 1998). It includes absorption and scattering by hydrometeors to calculate the expected microwave brightness temperatures corresponding to the atmospheric conditions simulated by the JMA-NHM.

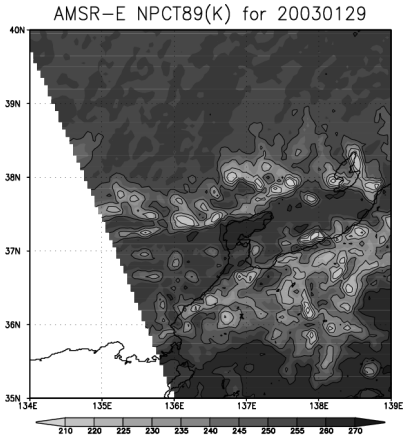

Fig. 2: Scattering index retrieved from 89 GHz brightness temperatures of AMSR-E at 13 JST on 29 January 2003.

Corresponding author's address: Hisaki Eito, Meteorological Research Institute, Japan Meteorological Agency, 1-1, Nagamine, Tsukuba, Ibaraki, 305-0052, Japan; E-Mail: heito@mri-jma.go.jp

4. RESULTS

Figure 3 shows a horizontal distribution of vertically integrated total condensed water simulated by the JMA-NHM. The JMA-NHM successfully reproduced features of broad cloud bands. In particular, model-simulated cloud bands resembled observed one (Fig. 1) in shape and location. Detailed features of several cloud streets were also simulated around cloud bands. Figure 4 shows a horizontal distribution of scattering index calculated from 89 GHz brightness temperature simulated by JMA-NHM and MRTM. The spatial structures of the simulated scattering index almost agree with that of AMSR-E observation (Fig. 2). However, the contrast between high and low scattering in simulation is stronger than that in AMSR-E observation. The magnitude of scattering index in simulation is much larger than that in observation. These results indicate that the JMA-NHM overestimated the amount of solid water particles. It is presented in the horizontal distributions of vertically integrated values of each solid water particles that most of model-simulated precipitation particles were snow particles(not shown). The maximum value of total snow water is ~ 6 kg m^{-2}. This value was almost equivalent to that of total precipitable water. In comparison with aircraft observations for each parameters of snow, JMA-NHM-simulated number concentrations (~ 100 /l) and averaged diameters (~ 0.5 mm) are almost reasonable. However, an amount of simulated water contents (~ 1.0 gm^{-3}) is larger than that in observation (~ 0.5 gm^{-3}). These gaps in the amount of snow between observation and simulation indicate the necessity of tuning and improvement of the cloud microphysics process in the JMA-NHM.

The same experiment was also conducted on the case in the previous day (not shown). In this case, cloud bands, of which cloud top height was about 3 km, were in the moderate stage. On the comparison of AMSR-E observation and numerical simulation, almost similar aspects shown in the developed case were also found in this case. However, a better agreement about a degree of the scattering was obtained between the simulation and the observation This result indicates that defferences of dvnamic structures such as the intensity of updraft and the cloud top height also affect the amount of model-simulated solid precipitation particles.

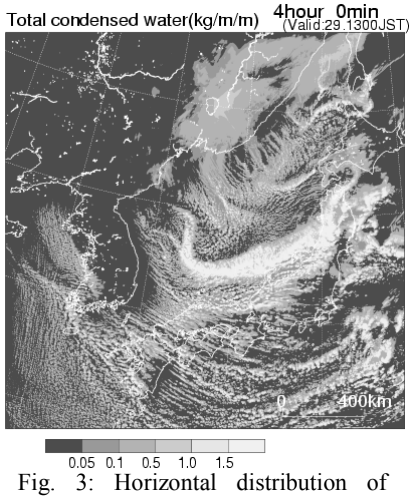

Fig. 3: Horizontal distribution of vertically integrated total condensed water simulated by the JMA-NHM (4 hour forecast).

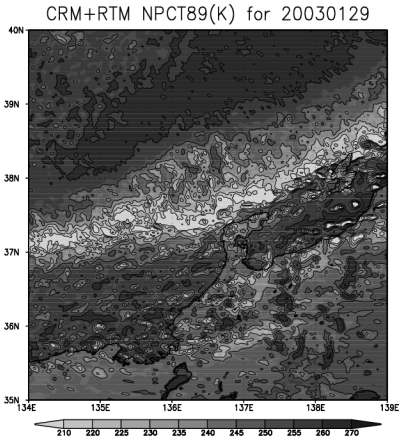

Fig. 4: Scattering index calculated from 89 GHz brightness temperatures simulated by MRTM with JMA-NHM -derived atmospheric conditions retrieved at 13 JST on 29 January 2003.

5. SUMMARY

A high-resolution wide-range numerical simulation of cloud bands observed on the Sea of Japan during the WAKASA2003 was performed using a CRM with 1km horizontal resolution and 2000 x 2000 km calculation domain. Cloud features observed by a meteorological satellite were well reproduced in CRM. Comparison of AMSR-E observation and simulation with CRM and MRTM suggests that CRM overestimates the amount of solid water particles, especially, snow particles. It is necessary to examine the process of cloud microphysics in the model and also to carry out the comparison with the other cases.

ACKNOWLEDGEMENTS

This study was supported by the fund of Japan Science and Technology Corporation - Core Research for Evolutional Science and Technology. The numerical calculations were made by the Earth Simulator.

REFERENCES

Liu G., 1998: A fast and accurate model for microwave radiance calculations. J. Meteor. Soc. Japan, **76**, 335-343.

Nagata M., M. Ikawa, S. Yoshizumi and T. Yoshida, 1986: On the formation of a convergence cloud band over the Japan Sea in winter; numerical experiments. J. Meteor. Soc. Japan, **64**, 841-855.

Nagata M., 1991: Further numerical study on the formation of a convergence cloud band over the Japan Sea in winter. J. Meteor. Soc. Japan, **69**, 419-428.

Nagata, M., 1992: Modeling case study of the Japan-Sea convergent cloud bands in a varying large-scale environment: evolution and upscale effect, J. Meteor. Soc. Japan, **70**, 649-671.

Saito, K., T. Kato, H. Eito and C. Muroi, 2001: Documentation of the Meteorological Research Institute/ Numerical Prediction Division Unified Nonhydrostatic Model. Tec. Rep. MRI, **42**, 133 pp.

NWP research in Austria

T. Haiden
Central Institute for Meteorology and Geodynamics
thomas.haiden@zamg.ac.at

1. Operational forecast system

Operational limited area weather forecasts in Austria are made using version AL25 of the ARPEGE/ALADIN modelling system. ALADIN forecasts are made on a Central European domain, with a horizontal resolution of 9.6 km, and 45 levels in the vertical. The model is spectral, run in hydrostatic mode, with a semi-implicit, semi-Lagrangian advection scheme. Initial and boundary conditions at 3-hourly intervals up to +48 hours are taken from the global model ARPEGE. The model is run twice per day. A modified Bougeault scheme is used for deep convection, a first-oder closure for turbulent vertical transports, and the ISBA (Interaction Soil-Biosphere-Atmosphere) scheme is used to represent surface processes.

2. Research

a. Numerical prediction of inversion fog and low stratus

The underprediction of low stratus capped by an inversion is a major NWP problem in eastern Central Europe. A negative bias in low cloud cover is among the primary sources of error in 2m temperature forecasts during wintertime. An empirical diagnostic inversion cloudiness scheme has been developed which scans the temperature and humidity profiles in the lower atmosphere for characteristic low stratus 'signatures'. If the signature is found, cloudiness is set to 1. Application of the scheme in ALADIN gives significantly improved low stratus forecasts, and, because of cloud-radiation feedback, improved diurnal temperature evolutions (Kann, 2003). With regard to valleys and basins it was found that in addition to using the scheme, horizontal diffusion of temperature must be set to small values in order to obtain a good low stratus forecast. This is because diffusion along sigma-type coordinate surfaces in a valley or basin tends to smooth inversions and allows vertical mixing to dry the PBL (Haiden, 2004a). The work is part of COST Action 722 'Short-Range Forecasting Methods of Fog, Visibility and Low Clouds'.

b. Prediction of cold air pools and katabatic flows

The fact that NWP models usually employ a terrain-following coordinate system at low levels poses a problem in the forecasting of cold air pools in complex terrain. Problems also occur as a result of the use of an envelope orography, such that cold air pools contained within alpine basins are generally not simulated well. In an ongoing research initiative, the mechanisms of katabatic flow formation and basin cooling at small scales are investigated in detail, using datasets from recent field experiments (Whiteman et al., 2004a,b; Haiden and Whiteman, 2004, 2005).

c. High-resolution analysis and nowcasting

A new high-resolution analysis and nowcasting system (INCA=Integrated Nowcasting through Comprehensive Analysis) is being developed at ZAMG. The system is three-

dimensional for temperature, humidity, and wind, and two-dimensional for precipitation. Horizontal resolution is 1 km, vertical resolution 100 m (z-type vertical coordinate). The time resolution and update frequency is 1 hour, except for precipitation where it is 15 minutes. The system takes a model forecast (operationally ALADIN) as a first guess. A three-dimensional error field is created by interpolating differences between the model forceast and observations at the station locations. Since there are a number of mountain stations, the error fields can be computed in 3-d mode. The interpolation of the point differences is done via geometric distance weighting in the horizontal, and potential temperature distance weighting in the vertical. The variables used are potential temperature and specific humidity, which are conserved for dry-adiabatic displacements. They will be replaced by liquid water potential temperature and total water content (conserved during pseudo-adiabatic displacements), in order to get good analyses of low clouds intersecting mountain slopes. Precipitation analyses are obtained from a combination of rain gauge and radar data, using a local regression and scaling approach. For the nowcasting of precipitation, motion vectors based on cross-correlation of previous subsequent analyses are used.

d. Limited area ensemble forecasting

Limited are models provide highly structured forecast fields both in space and time. However, often the small-scale features are extremely sensitive to uncertainties of the model and/or initial conditions. To obtain a guidance for the forecaster with regard to this uncertainty, the project "ALADIN Limited Area Ensemble Forecasting" has been started at ZAMG. It is an ensemble forecast system with 11 members, in which perturbed initial conditions are created using a breeding method. In a second step, the ensemble transform Kalman filter (ETKF) technique will be applied to the breeding vectors. The NWP model used is ALADIN with reduced horizontal and vertical resolution (16 km, 31 levels). The domain covers the whole of Europe and large parts of the North Altantic.

References

Haiden, T., 2004a: Improvement of low stratus forecasts. Proceedings, *13th ALADIN Workshop*, Prague.

Haiden, T., and C. D. Whiteman, 2004: Processes leading to inversion buildup in small enclosed basins. Preprints, *11th Conference on Mountain Meteorology*, Amer. Meteor. Soc., New Hampshire.

Haiden, T., 2004b: Mixed layers with steep topography. *Bull. Am. Met. Soc.*, **85,** 946.

Haiden, T., and C. D. Whiteman, 2005: Katabatic flow mechanisms on a low-angle slope. *J. Appl. Meteor.*, **44,** (in press).

Kann, A., 2003: 1 month parallel run with Seidl-Kann cloudiness scheme. ALADIN Newsletter 24.

Kann, A., and T. Haiden, 2005: The August 2002 flood in Austria: sensitivity of precipitation forecast skill to area size and duration. *Meteorol.Z.*, **14,** (submitted).

Whiteman, C. D., T. Haiden, B. Pospichal, S. Eisenbach and R. Steinacker, 2004: Minimum temperatures, diurnal temperature ranges and temperature inversions in limestone sinkholes of different size and shape. *J. Appl. Meteor.*, **43,** 1224-1236.

Whiteman, C. D., S. de Wekker, and T. Haiden, 2004: Boundary layer moisture regimes in small closed basins. Preprints, *16th Symp. on Bound. Layers and Turbulence* , Amer. Meteor. Soc., Portland.

Implementation of Targeted Moisture Diffusion for the JMA Regional Spectral Model (RSM)

Takuya Hosomi

Numerical Prediction Division, Japan Meteorological Agency

1-3-4 Otemachi, Chiyoda-ku, Tokyo 100-8122, JAPAN

hosomi@met.kishou.go.jp

Japan Meteorological Agency operates the Regional Spectral Model (RSM) twice a day. It covers East Asia and makes a forecast up to 51 hours. A forecast of the JMA Global Spectral Model (GSM) is used for a lateral boundary condition. An initial condition is analyzed by a regional four-dimensional variational data assimilation (4D-Var) system (Shimbori and Koizumi 2004).

Occasionally RSM predicts a pseudo small low on the sea, usually with a locally strong upward motion and an intense rainfall. The Targeted Moisture Diffusion (TMD) can suppress such a grid-scale storm through applying a second order horizontal diffusion for water vapor around the storm selectively (Stainforth et al. 2003). It works on a grid where an upward motion is bigger than a certain threshold. After some sensitivity tests, -90 hPa/hour of a vertical-p velocity is choosed as the threshold.

To confirm the impact of the scheme, two series of forecast experiments were carried out for a couple of weeks in July 2003 and January 2004. As a result of these experiments, it is found that a tendency of predicting the pseudo small low on the sea is reduced in winter (Fig 1). The new scheme also improves a regional analysis field through an improved first guess field (6hour forecast of the model) (Fig 2). A statistical verification shows that the root mean square error (RMSE) of sea level pressure forecasts is improved in January 2003 (Fig 3). The threat score of precipitation forecasts is also shown in Fig.3. The score for the new RSM is almost equal to the former RSM.

The JMA has implemented TMD in operational RSM in April 2004.

Reference

Shimbori, T. and K. Koizumi, 2004: Operational implementation of the JMA Regional Four-Dimensional Variational Data Assimilation System. Research Activities in Atmospheric and Oceanic Modelling, No.34, WMO/TD-No.1220, 01.31-01.32.

Stainforth et al. 2003: Unified Model Documentation Paper 15 (Joy of New Dynamics) (UM5.5) (not published).

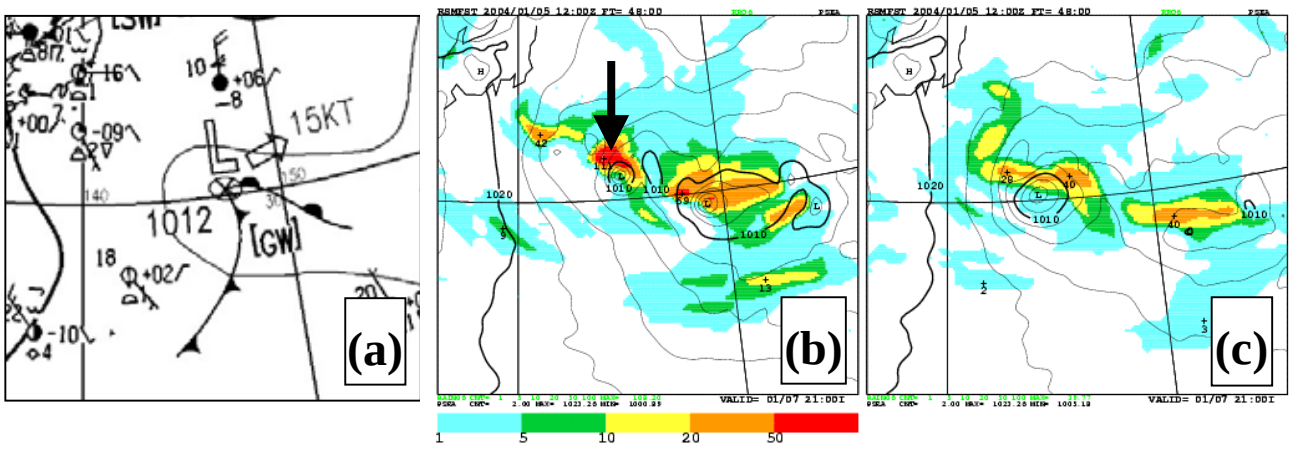

Fig 1 Surface level pressure at 12UTC Jan 07 2004. (a) Subjective analysis, (b) 48 h forecast without TMD (CNTL), (c) 48 h forecast by RSM with TMD (NEW). Predicted rain areas are shaded. TMD suppresses the grid-scale storm denoted by an arrow and the associating heavy rain in CNTL.

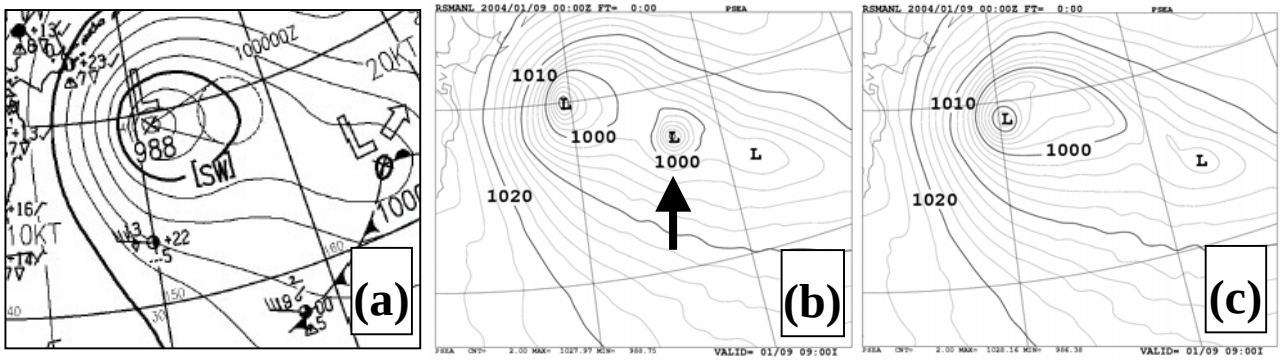

Fig 2 Surface level pressure at 00UTC Jan 09 2004. (a) Subjective analysis, (b) Regional analysis without TMD (CNTL), (c) Regional analysis with the first guess field made by RSM with TMD (NEW). A pseudo low in the CNTL analysis denoted by an arrow disappears in the NEW analysis.

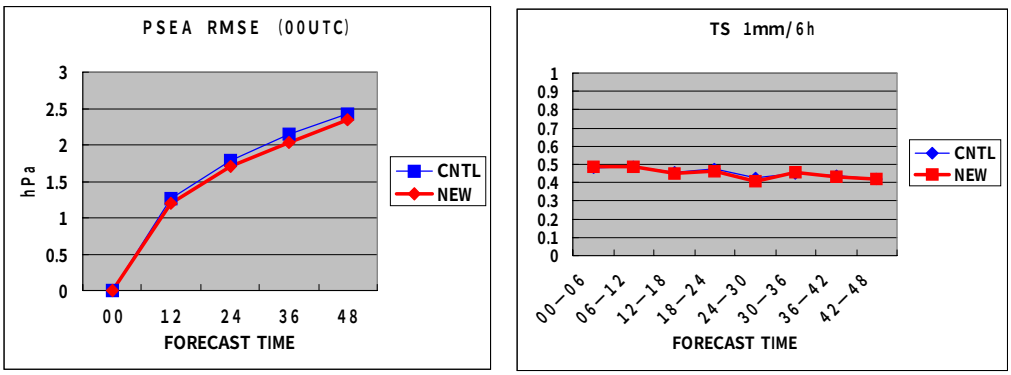

Fig3 (left) RMSE of sea level pressure. (right) Threat score of 1mm/6h precipitation forecasts. Thin line is for CNTL, bold line is for NEW.

Verification of mesoscale forecasts by the newly implemented JMANHM

Jun-ichi Ishida and Saori Tanaka
Numerical prediction Division, 1-3-4 Otemachi, Chiyoda-ku, Tokyo 100-8122, Japan
E-mail: j_ishida@met.kishou.go.jp, s-tanaka@naps.kishou.go.jp

1. Introduction

The Japan Meteorological Agency (JMA) started operating a numerical prediction system for disaster prevention in March 2001 using a hydrostatic model (MSM) with a horizontal resolution of 10 km. A nonhydrostatic model (NHM) has been developed based on the MRI/NPD unified nonhydrostatic model (Saito et al., 2001) in collaboration with the Meteorological Research Institute, and put into operation on 1 September 2004 in place of MSM.

2. Specifications of the operational NHM

The forecast domain of NHM covers the Japan Islands and surrounding areas with grid points of 361 x 289 at a horizontal resolution of 10 km, and the model is integrated up to 18 hours four times a day. The initial fields are prepared by the JMA mesoscale 4D-Var analysis based on MSM. Since the 4D-VAR analysis does not produce the initial fields of the water substances except water vapor, guessed values for these variables are taken from the outputs of the preceding forecast (Ishida and Saito, 2005). The lateral boundary conditions are given by the forecast from the JMA regional model with a grid spacing of 20 km. The model topography of NHM is made from GTOPO30 developed by the U.S. Geological Survey.

The governing basic equations of NHM are fully compressible equations with conformal map factors. Terms responsible for sound waves and gravity waves are treated implicitly in the vertical direction and explicitly in the horizontal (HE-VI, time splitting scheme), where long and short time steps are 40 and 80/7 seconds, respectively. The fourth order scheme is chosen for horizontal advection considering accuracy and computational efficiency (Fujita, 2003). To enhance the computational stability the lower (second order) components of the advection terms are adjusted at each short time step only in the later half of the leap-frog time integration (Saito, 2003) and the modified centered difference advection scheme (Kato, 1998) is used.

A three-ice bulk microphysics scheme was implemented, and some trivial processes are omitted for computational efficiency (Yamada, 2003). The Kain-Fritsch cumulus convection scheme (Kain and Fritsch, 1993) is employed with some parameters changed to suit operational run with 10 km mesh (Ohmori and Yamada, 2004). The non-local effect is considered in the planetary boundary layer scheme (Kumagai, 2004).

The details of the above mentioned scheme and other features are described in Saito et al.(2005).

3. Verification results

In this section, the performance of NHM is shown in comparison with MSM for the period of April to August 2004. The rainfall prediction is verified against rader-rain gauge composite data. Figure 1 shows the time sequences of bias and threat scores for three hour precipitation by NHM and MSM. The verifications are carried out for every 20 km square mesh and for grids over land and over sea nearby the coast. The threat scores of NHM are mostly equal to those of MSM for threshold value 1mm/3hr, and moderately better for 10mm/3hr, while the bias scores of NHM are almost same as those of MSM for both of the threshold values.

Figure 2 shows root mean square error of the 18-hour predicted fields by NHM and MSM against radiosonde observations. Verifications are done for the zonal wind field (left top), for the meridional wind field (right top), for the temperature field (left bottom), and for the relative humidity field (right bottom). The performance of NHM is comparable with that of MSM except that NHM performs better than MSM in the upper troposphere and the lower stratosphere, especially for the relative humidity field.

4. Concluding Remarks

The development of the model is continued for further improvement of the model dynamics and physics. The mesoscale numerical prediction system will be enhanced in terms of the horizontal resolution and frequency of operation after the replacement of the computer system in March 2006.

Acknowledgement

The Kain-Fritsch scheme was developed with reference to the Weather Research and Forecast Model by the courtesy of Dr. Jack Kain and Dr. Jimmy Dudhia.

References.

Fujita, T., 2003: Higher order finite difference schemes for advection of NHM. *Proceedings, International Workshop on NWP Models for Heavy Precipitation in Asia and Pacific Areas,* 78-81.

Ishida, J. and Saito K., 2005: Initialization Scheme for Water Substances in the operational NHM. *CAS/JSC WGNE Res. Act. in Atmos. and Ocea. Modelling.* (to be submitted)

Kain J. and J. Fritsch, 1993: Convective parameterization for mesoscale models: The Kain-Fritsch scheme. The Representation of Cumulus Convection in Numerical Models, Meteor. Monogr., **24**, 165-170.

Kato T., 1998: Numerical simulation of the band-shaped torrential rain observed southern Kyushu, Japan on 1 August 1993. *J. Meteor. Soc. Japan,* **76**, 97-128.

Kumagai, Y., 2004: Implementation of a non-local like PBL scheme in JMANHM. *CAS/JSC WGNE Res. Act. in Atmos. and Ocea. Modelling.* **34**, 0417-0418.

Ohmori, S. and Y. Yamada, 2004: Implementation of the Kain-Fritsch Convective Parameterization scheme in the JMA's Non-hydrostatic Model. *CAS/JSC WGNE Research Activities in Atmospheric and Oceanic Modelling.* **34**, 0425-0426.

Saito, K., 2003: Time-splitting of advection in the JMA Nonhydrostatic Model. *CAS/JSC WGNE Res. Act. in Atmos. and Ocea. Modelling.* **33**, 0315-0316.

Saito, K., T. Fujita, Y. Yamada, J. Ishida, Y. Kumagai, K. Aranami, S. Ohmori, R. Nagasawa, S. Tanaka, C. Muroi, T. Kato and H. Eito, 2005: The operational JMA Nonhydrostatic Mesoscale Model. *Mon. Wea. Rev*. (to be submitted)

Saito, K., T. Kato, H. Eito and C. Muroi, 2001: Documentation of the Meteorological Research Institute/Numerical Prediction Division unified nonhydrostatic model. *Tec. Rep. MRI,* **42**, 133pp.

Yamada, Y., 2003: Cloud microphysics, *Separate volume of annual report of NPD,* **49**, 52-76. (in Japanese)

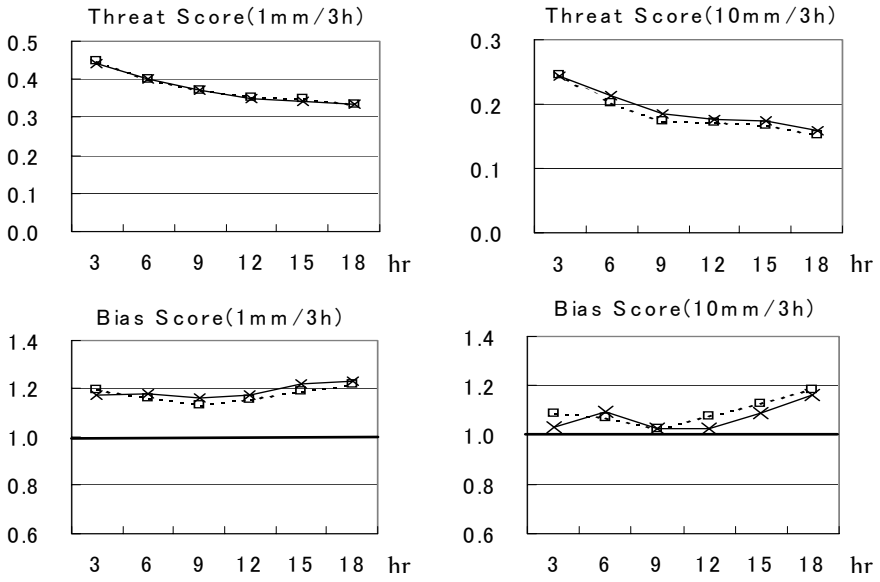

Fig. 1 Time sequences of threat and bias scores for three hour precipitation.
The solid line indicates NHM and the dashed line indicates MSM.

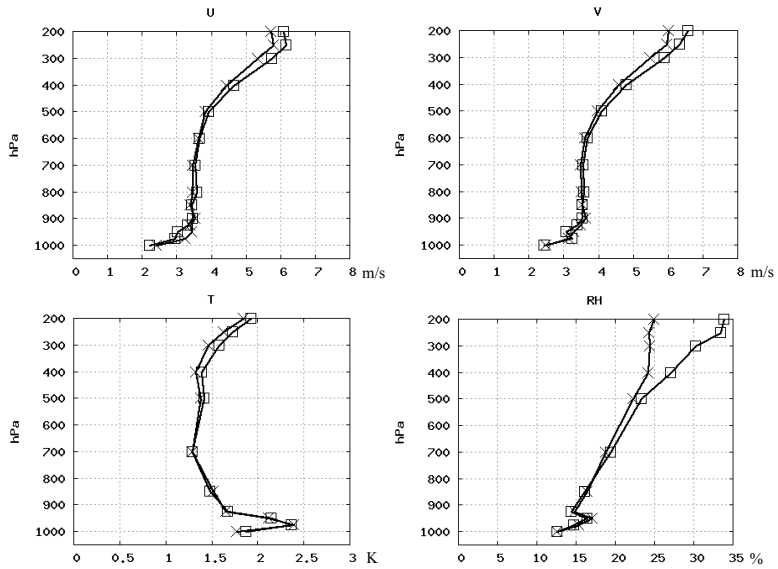

Fig. 2 RMSE of 18 hr forecasts from NHM (×) and MSM (□) against radiosonde. Verifications are carried out for the zonal wind field (left top), for the meridional wind field (right top), for the temperature field (left bottom), and for the relative humidity field (right bottom).

Prediction of Localized Heavy Rainfall using a Cloud-resolving Nonhydrostatic model and its Problems

Teruyuki KATO* and Kohei ARANAMI**

*Meteorological Research Institute / Japan Meteorological Agency, Tsukuba
**Numerical Division / Japan Meteorological Agency, Tokyo

During the Baiu season, localized heavy rainfall is often observed over the Baiu frontal zone. On 13 and 18 July 2004, heavy rainfalls causing serious floods occurred in Niigata and Fukui areas, Japan-Sea side of Japan Islands, respectively. For both events, band-shaped precipitation systems with the length larger than 100 km stagnated for about 12 hours, and they caused over 200mm accumulated precipitation (see Fig. 1 for Niigata event). These heavy rainfalls were brought by the enhancement of convective instability over the Baiu front that was resulted from the inflows of low-level humid air and middle-level dry air (Figs. 2a and 2c). The humid air had moved over the sea around the edge of Pacific high pressure zone, while the origin of the dry air was downdraft air over the Chinese continent. Therefore, the dry air was considerably warmer, not colder than the surrounding atmosphere (Fig. 2b).

Numerical simulations in an attempt to reproduce these heavy rainfall events were carried out using a cloud resolving model with a horizontal grid of 1.5 km and 5 km, Japan Meteorological Agency (JMA) nonhydrostatic model (1.5km-NHM and 5km-NHM). The initial conditions of 5km-NHM were produced from the JMA mesoscale analysis with a four-dimensional variational assimilation technique. 1.5km-NHM was nested within the forecasts of 5km-NHM. In both NHMs, microphysics with the ice phase are used as precipitation processes, and the Kain-Fritsch convective parameterization scheme is also used conjunctionally in the 5km-NHM.

For Niigata event, Mesoscale model of JMA with a horizontal grid of 10 km (MSM) predicted some rainfall areas around Niigata area, but they were not band-shaped (Fig. 1b). Prediction with a 5km-NHM (Fig. 1c) was not enough to reproduce the band-shaped structure. However, 1.5km-NHM successfully predicted a band- shaped rainfall area (Fig. 1d), although the predicted precipitation intensity was weaker than the observation. This success could result from the 1.5km-NHM being able to reproduce a life cycle of cumulonimbus with a one-hour lifetime.

Even when 1.5km-NHM was applied to Fukui event, any heavy rainfall area was not predicted. This indicates that a cloud-resolving model can not reproduce this event, when a coarse resolution model (e.g., MSM) predicts little precipitation around the area where heavy rainfall was observed. The reason of this failure may be resulted from the uncertain analysis over the sea due to no upper sounding observation. The heavy rainfall, observed over the area marked by a bold circle in Fig. 3b, was caused by the inflow of low-level humid air. This low-level humid air was traced back to the area marked by a dashed cycle in Fig. 3a before 12 hours. The humid air with specific humidity exceeding 16 g kg^{-1}, enough to bring heavy rainfall, did not reach the Fukui area in the MSM prediction (Fig. 4). Therefore, the 1.5km-NHM failed to predict the heavy rainfall due to an inaccurate analysis of the low-level wind field over the sea that determined the movement of the humid air inducing the heavy rainfall.

The paths of the low-level humid air and middle-level dry air bringing heavy rainfall are examined. Since the Japan Islands are surrounded by the sea, these air flows must pass over the sea before reaching the islands. However, since upper-air sounding is seldom operated over the sea, it is difficult to make a highly accurate analysis of atmospheric conditions there. Kato et al. (2003) pointed out that the analysis of water vapor is most difficult because it is independent from the other observed variables. Furthermore, such a slight mistake in the analyzed wind field, as found in the Fukui case, may cause false prediction of heavy rainfall. It is noted that an analysis over areas where no observation is available is mainly made from the uncertain forecasts using the previous initial conditions. Therefore, this study suggested that new systems are required to accurately observe the atmospheric conditions over the sea.

*Corresponding authors address: Teruyuki KATO, Meteorological Research Institute, 1-1 Nagamine, Tsukuba, Ibaraki 305-0052, Japan

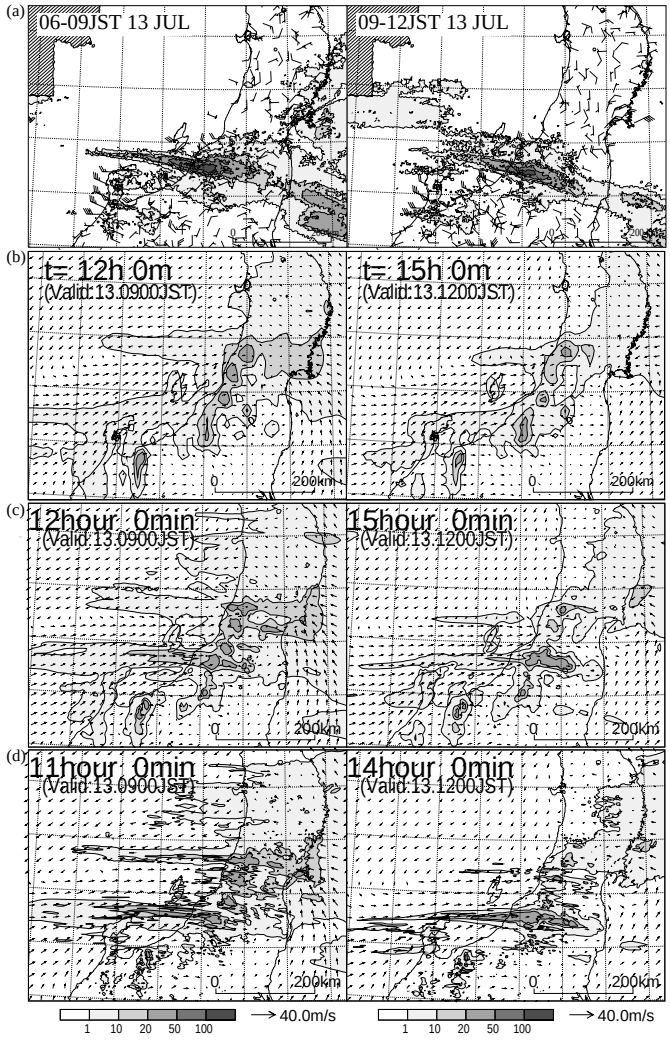

Fig. 1 (a) Observed 3 hourly accumulated rainfall chart on 13 July 2004. Arrows show the observed surface winds. Same as (a), but (b) MSM, (c) 5km-NHM, (d) 1.5km-NHM prediction.

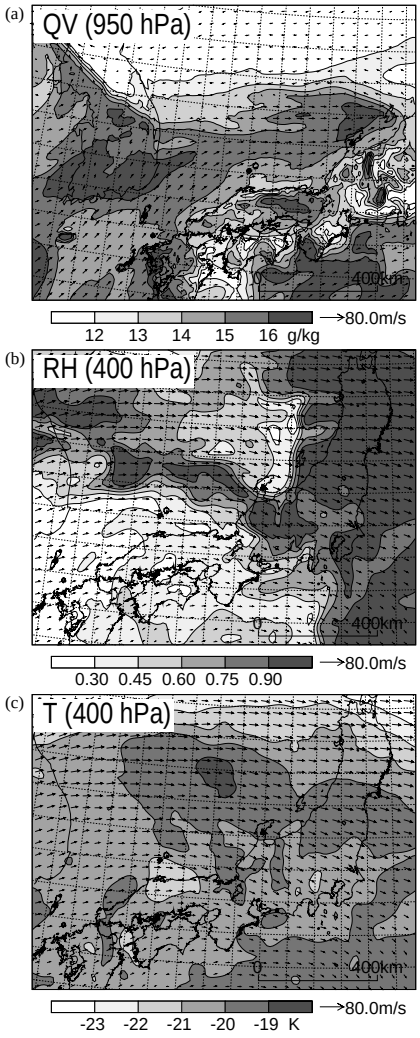

Fig. 2 (a) 950hPa-level specific humidity, 400hPa-level (b) temperature, and (c) relative humidity field at 09 JST on 13 July 2004. Vectors show the same level horizontal winds.

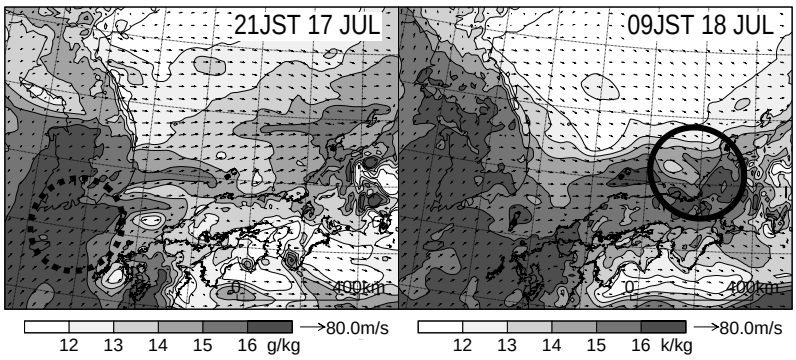

Fig. 3 950hPa-level specific humidity fields of JMA mesoscale analyses at 21 JST 17 July and 09 JST 18 July 2004. Vectors show the same level horizontal winds.

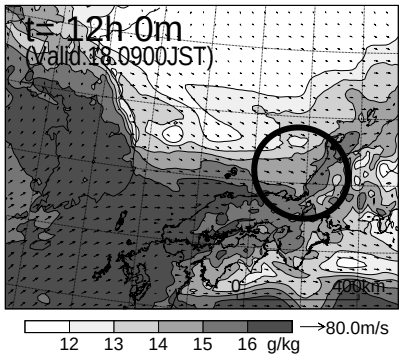

Fig. 4 Same as right panel of Fig. 3, but prediction of MSM.

REFERENCE

Kato, T., M. Yoshizaki, K. Bessho, T. Inoue, Y. Sato and X-BAIU-01 observation group, 2003: Reason for the failure of the simulation of heavy rainfall during X-BAIU-01- Importance of a vertical profile of water vapor for numerical simulations – *J. Meteor. Soc. Japan*, **81**, 993-1013.

Kato, T., and K. Aranami, 2005: Formation factors of 2004 Niigata-Fukushima and Fukui heavy rainfalls and problems in the predictions using a cloud-resolving model, *SOLA*, **1**, 1-4.

Tropical Cyclone Intensity Change in a Uniform Flow

Joey H. Y. Kwok and Johnny C. L. Chan*
Laboratory for Atmospheric Research, Dept. of Physics & Materials Science
City University of Hong Kong, Hong Kong, China
*Email: Johnny.Chan@cityu.edu.hk

1. Introduction

In recent tropical cyclone (TC) modeling studies, much efforts have been devoted to the effect of environmental vertical wind shear on TC intensity change (e.g. Bender 1997; Frank and Ritchie 1999, 2001; Wong and Chan 2004). It is generally concluded that the vertical wind shear has a negative impact for TC intensification. However, discrepancies of results are found for a simple case of a TC under the influence of a uniform flow. Frank and Ritchie (2001) found that a TC in a 3.5 m s^{-1} uniform background flow slightly intensifies compared with a no-flow case while Peng et al. (1999) showed that a TC weakens in a uniform flow of 5-10 m s^{-1}. This study therefore attempts to investigate the effect of uniform flow on TC intensity changes.

2. Model configuration

The Pennsylvania State University / National Center of Atmospheric Research Mesoscale Model version 5 (MM5) is used in this study. The domain size is 301 x 301 grid points with 24 sigma levels, and the grid resolution is 15 km. The Betts-Miller (Betts and Miller 1986) cumulus parameterization scheme is used to spin-up the vortex for 24 h of model time. Uniform flow with 0 – 8 m s^{-1} is imposed on both *f* and beta planes with the Betts-Miller scheme turned off.

3. Results

A stronger uniform flow imposed on an *f* plane results in a weaker vortex (Fig. 1a), which is due to the development of vertical wind shear induced by an asymmetry in vertical motion. Wavenumber-1 asymmetries in vertical motion and a rotation of the upper-level anticyclone appear to reduce the secondary circulation of the vortex, which introduces a vertical wind shear. The induced vertical wind shear further weakens the secondary circulation of the vortex as described by Wong and Chan (2004) so that the vortex under a strong uniform flow weakens with time. For a weak uniform flow, the asymmetric vertical motion is not strong enough to reduce the secondary circulation so that vertical wind shear cannot develop.

For the cases on a beta plane, the TC in the no-flow case weakens significantly by the beta-induced shear relative to that on an *f* plane. Moreover, a westerly flow is more favorable for TC intensification than easterly flow (Fig. 1b). It is because the beta-induced shear vector is towards the southeast, so a westerly uniform flow enhances TC development by canceling part of the beta-induced shear whereas an easterly flow strengthens it by altering the magnitude and direction of the shear vector (Fig. 2).

Acknowledgments. The authors would like to thank Mr. Martin Wong for helpful discussions. This research is sponsored by the Research Grant Council of the Hong Kong Special Administrative Region, China Grant CityU 1050/02P.

4. References

Bender, M. A., 1997: The effect of relative flow on the asymmetric structure if the interior of hurricanes. *J. Atmos. Sci.,* **54**, 703-724.

Betts, A.K. and M. J. Miller, 1986: A new convective adjustment scheme. Part II: A new convective adjustment scheme, Part II: Single column tests using GATE wave, BOMEX, ATEX and arctic air-mass data sets. *Quart. J. Roy. Meteor. Soc.*, **112,** 693-709.

Frank, W. M., and E. A. Ritchie, 2001: Effects of vertical wind shear on the intensity and structure of numerically simulated hurricanes. *Mon. Wea. Rev.*, **129,** 2249-2269.

Peng, M. S., B. F. Jeng, and R. T. Williams, 1999: A numerical study on tropical cyclone intensification. Part I: Beta effect and mean flow effect. *J. Atmos. Sci.*, **56,** 1404-1423.

Wong, M. L. M. and J. C. L. Chan, 2004: Tropical cyclone intensity in vertical wind shear. *J. Atmos. Sci.*, **61,** 1859-1876.

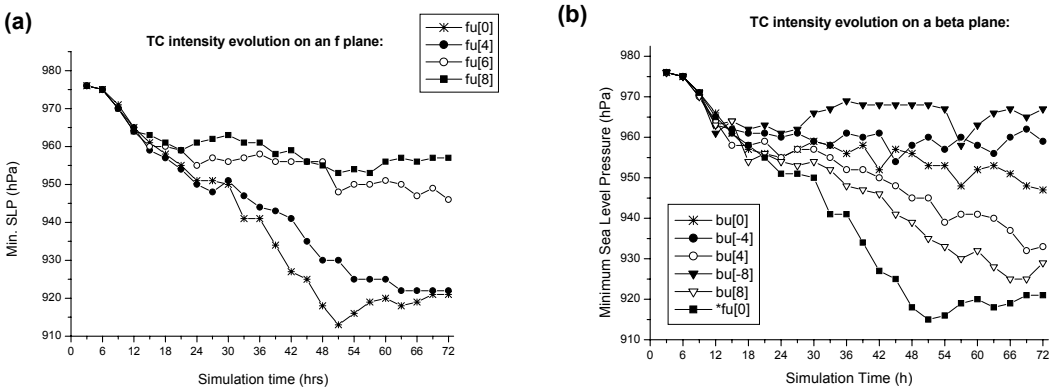

Fig. 1. Intensity evolution of vortices on (a) f plane and (b) beta plane, (symbol fu[x] & bu[x] represent f-plane and beta-plane experiments respectively, the number insides the brackets denote the uniform flow speed, positive number indicates a westerly flow while negative number indicates an easterly flow).

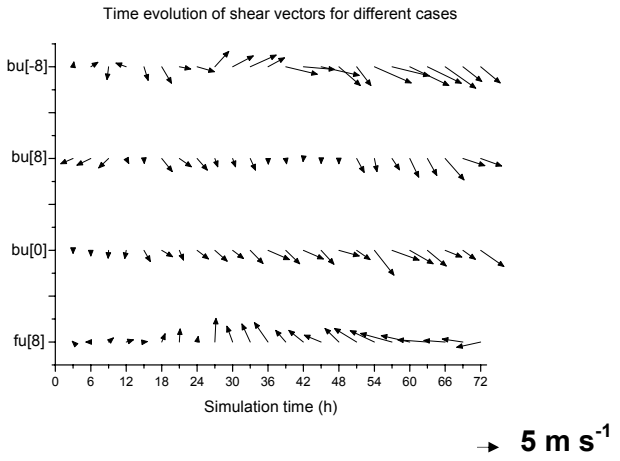

Fig. 2. Time evolution of the vector shear for the fu[8], bu[0], bu[8] and bu[-8] cases respectively.

Development of a high-resolution meso-scale model at JMA

Hiroshi Nakayama and Kohei Aranami
Numerical Prediction Division, Japan Meteorological Agency
1-3-4 Otemachi, Chiyoda-ku, Tokyo 100-8122, Japan
h-nakayama@naps.kishou.go.jp, aranami@naps.kishou.go.jp

1 Introduction

The Japan Meteorological Agency (JMA) has been operating the JMA nonhydrostatic model (NHM) with a horizontal resolution of 10-km since 1 September 2004, and is planning to enhance the horizontal and vertical resolution of the model. Preliminary experiments are conducted with a 5-km NHM, which has been developed for next computer system introduced in March 2006. Tests of even higher-resolution models are also carried out to examine the prospects of very high-resolution simulations.

2 Simulation of 2004 Niigata/Fukushima heavy rainfall

A heavy rainfall event occurred over Niigata/Fukushima area on 13 July 2004. A 5-km mesh simulation was attempted for this case by using the same initial and boundary conditions as those used in the operational model forecast. The specifications of the model simulation are shown in Table 1, and the initial time of the forecast is 12 UTC, 12 July 2004. Figure 1 shows the predicted precipitation by the operational model (left), the 5-km model (center) and from T+9 to T+12 along with the corresponding Rader-AMeDAS data[1](right). Although the precipitation intensity of the model simulations is not as strong as observation, the band-shaped structure is reproduced more realistically in the 5-km simulation than in the 10-km. We conclude that the horizontal resolution plays a very important role for the simulation of the meso-scale rain band.

Table 1: Specifications of the model simulation

Initial time	12UTC 12 July 2004
Forecast time	18 hours
Number of grid points	$719 \times 575 \times 50$
Horizontal resolution	5 km
Vertical resolution	40-904 m
Time step	24 seconds
Time integration	split-explicit methods
Advection scheme	horizontally 4th order centered flux form
Prognostic variables	$U, V, W, p, \theta, qv, qc, qr, qi, qs, qg$

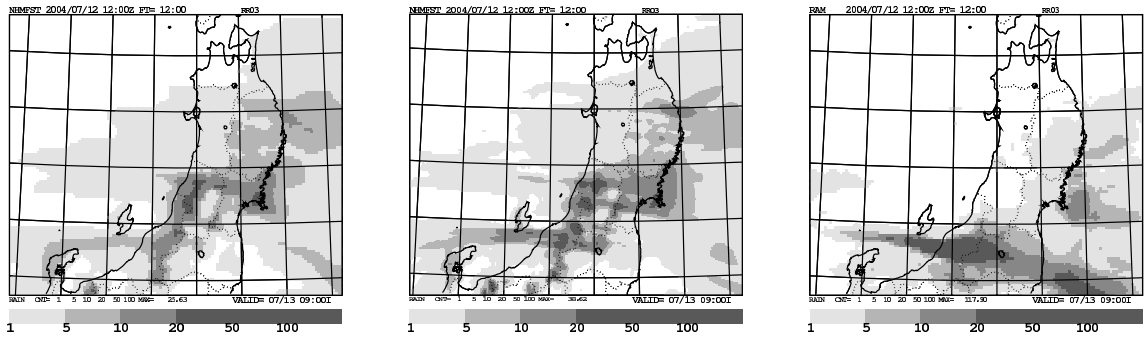

Figure 1: The simulation result of 2004 Niigata/Fukushima heavy rainfall. Left:The result of operational NHM. Center: The result of 5km NHM. Right: The Radar-AMeDAS precipitation. Three-hour accumulated precipitation is presented. The initial time is 12 UTC, 12 July 2004.

[1]Rader-rain gauge composite rainfall data.

3 High-resolution model simulations for the typhoon T0406

JMA has been investigating the usability of model simulation at very high resolution for detailed aviation weather information in a joint research with the Japan Aerospace Exploration Agency (JAXA). The simulations are made for a case of the typhoon T0406 on 21 June 2004 by using NHM. The simulations were conducted with 5-km, 2-km and 500-m horizontal resolutions. The initial and boundary conditions of 5-km NHM are provided by the operational system of JMA, and those for higher-resolution models are by the coarser models.

Table 2 shows the specifications of the simulations. The forecast domain and the prediction of sea surface pressure, surface wind and rainfall at 06 UTC on the day of each simulation are presented in Figure 2.

Table 2: Specifications of the simulations

Resolution	5 km	2 km	500 m
Initial condition	MANAL[2]	5-km NHM	2-km NHM
Boundary condition	RSM	5-km NHM	2-km NHM
Grid size	719 ×575 ×50	500 ×500 ×60	500 ×500 ×60

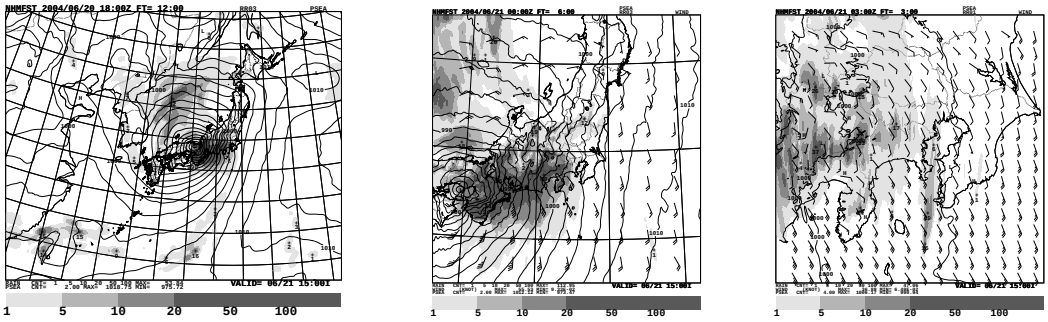

Figure 2: Sea surface pressure, surface wind and rainfall at 06 UTC, 21 June 2004 simulated by NHM. Left: 5-km NHM. Center: 2-km NHM. Right: 500-m NHM.

Figure 3 shows the simulated and observed changes of wind speed from 03 to 10 UTC on the day at Kofu City, which is located in the mountain area in Central Japan. The 500-m NHM roughly corresponds with the observation in predicting the intensification around 04, 07 and 09 UTC while the lower resolution simulations do not show that tendency. Figure 4 presents the mean error of surface wind speed for all the surface observation sites in the forecast domain. The finer resolution model yields smaller mean error.

Further analyses of the case and testing of the model are still continued.

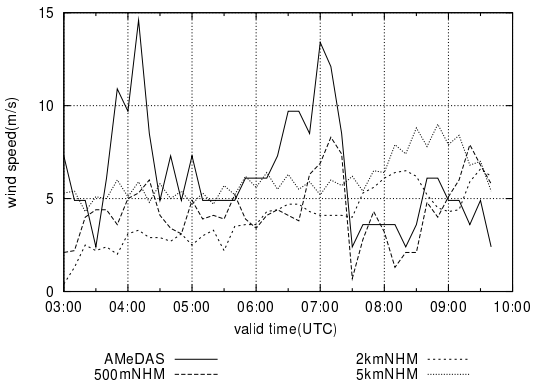

Figure 3: Time series of the wind speed at Kofu.

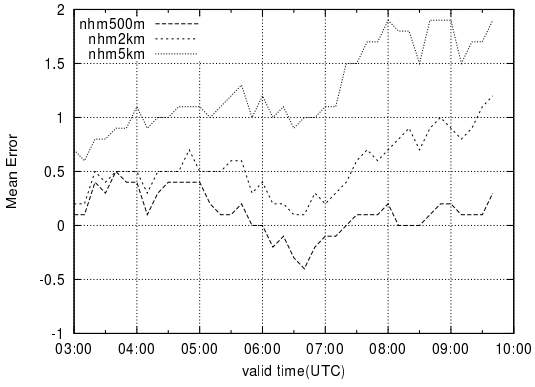

Figure 4: Time series of the mean error of wind speed for all the observation sites.

[2]Operational analysis for the meso-scale model at JMA.

Implementation of the Targeted Moisture Diffusion to JMA-NHM

Kazuo Saito* and Jun-ichi Ishida**
** Meteorological Research Institute, Tsukuba, Ibaraki 305-0052, Japan; ksaito@mri-jma.go.jp*
*** Numerical Prediction Division, Japan Meteorological Agency*

The Japan Meteorological Agency (JMA) started the operational run of a nonhydrostatic model ('JMA-NHM'; hereafter simply mentioned as 'NHM') on 1 September 2004 in place of the former operational hydrostatic mesoscale model of JMA (MSM). NHM is a community nonhydrostatic model for both operational NWP and research, whose original root is based on the Meteorological Research Institute/Numerical Prediction Division unified nonhydrostatic model (Saito et al. 2001).

As for the moist physical processes, the Kain-Fritsch (K-F) parameterization scheme has been implemented in addition to the bulk cloud microphysics. Several modifications have been done to improve its performance in a 10 km resolution NWP, especially for prediction of heavy rainfall events in Japan where moist and unstable maritime air-mass prevails (Ohmori and Yamada, 2004). One of the modifications is the "closure assumption", where the default setting assumed that the convection consumes the pre-existing CAPE by 90 % in a single application of the K-F scheme. However, forecast experiments showed that this setting tended to over-stabilize the model atmosphere, and strong rain decreased with time in the forecast period. To prevent this undesirable excessive stabilization of the model atmosphere, CAPE left in the column after a single application of the K-F scheme was increased from the default value (10 %) to 15 %. With this modification, heavy rainfall events were well reproduced by NHM compared with NHM using the original K-F scheme and MSM. However, on the other hand, intense grid scale updrafts often developed in the model with this increased rate of residual CAPE, because this change allows more convective unstableness in the model atmosphere.

In order to control the grid point storms and the associated intense grid scale precipitation, the targeted moisture diffusion (TMD) has been newly implemented to NHM. The basic idea of TMD was developed by Dr. Terry Davies of the UK Met Office for the Unified Model (UM; Staniforth et al., 2004), where a second order horizontal diffusion is applied to water vapor when strong upward motions exist to selectively damp the grid point storms and associated intense grid scale precipitation. In the mesoscale UM with 38 levels and a horizontal resolution of 0.11 deg (12km), TMD is applied to all grid points in a column where the upward motion exceeds 1.0 m/s. In case of NHM, horizontal diffusion with an *e*-folding time of 300 sec is applied to water vapor at grid points where the upward motion exceeds 2.0 m/s.

Figure 1 shows an example of time sequence of the maximum updraft and rainfall intensity by NHM which covers the MSM domain. The initial time is 18 UTC 18 July 2003. Without TMD, the maximum updraft reaches 6 m/s at FT=5-8hr, and very intense rains about 140 mm/hr are predicted at FT=7-8hr. At FT=16.8hr, a spike-like strong updraft of 8 m/s is seen, which is caused by grid point deep convection. With TMD, the maximum updraft and the maximum rain intensity are reduced to reasonable values, less than 4.5 m/s and 80 mm/hr, respectively. Figure 2 shows the one hour precipitation at 02 UTC 19 July 2003 predicted by NHM with and without TMD. As seen in this figure, major precipitation pattern is not affected by the inclusion of TMD. Figure 3 shows the histogram of 1 hour precipitation intensity for the model grid of NHM. TMD effectively reduces the over-intense precipitation greater than 50 mm/hr without changing the weak to moderate rains. TMD has been implemented to the JMA new operational nonhydrostatic mesoscale model (Saito et al., 2005).

References

Ohmori, S. and Y. Yamada, 2004: Implementation of the Kain-Fritsch Convective Parameterization scheme in the JMA's Non-hydrostatic Model. *CAS/JSC WGNE Research Activities in Atmospheric and Oceanic Modelling*. **34**, 0425-0426.

Saito, K., T. Fujita, Y. Yamada, J. Ishida, Y. Kumagai, K. Aranami, S. Ohmori, R. Nagasawa, S. Tanaka, C. Muroi, T. Kato and H. Eito, 2005: The operational JMA Nonhydrostatic Mesoscale Model. *Mon. Wea. Rev.* (to be submitted)

Saito, K., T. Kato, H. Eito and C. Muroi, 2001: Documentation of the Meteorological Research Institute/Numerical Prediction Division unified nonhydrostatic model. *Tec. Rep.* MRI, **42**, 133pp.

Staniforth, A., A. White, N. Wood, J. Thuburn, M. Zerroukat, E. Cordero et. al., 2004: Joy of U.M. 6.0 - Model Formulation, *Unified Model Documentation Paper*, **15**, UKMO.

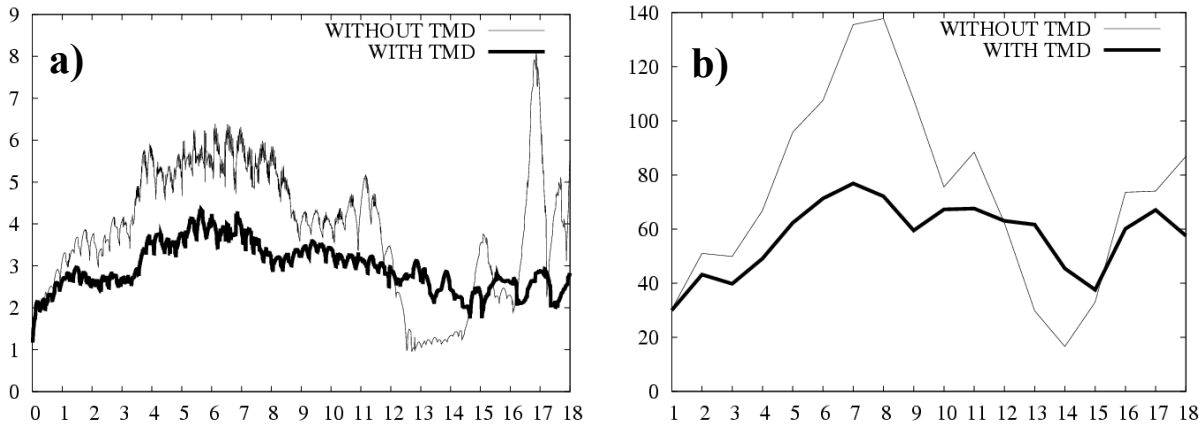

Fig. 1. a) Time sequence of the maximum updraft in a simulation with and without TMD. Initial time is 18 UTC 18 July 2003. Units of horizontal and vertical axes are hr and ms^{-1}, respectively. **b)** Same as in a) but the maximum one hour rain intensity. Unit of vertical axis is mm/hr.

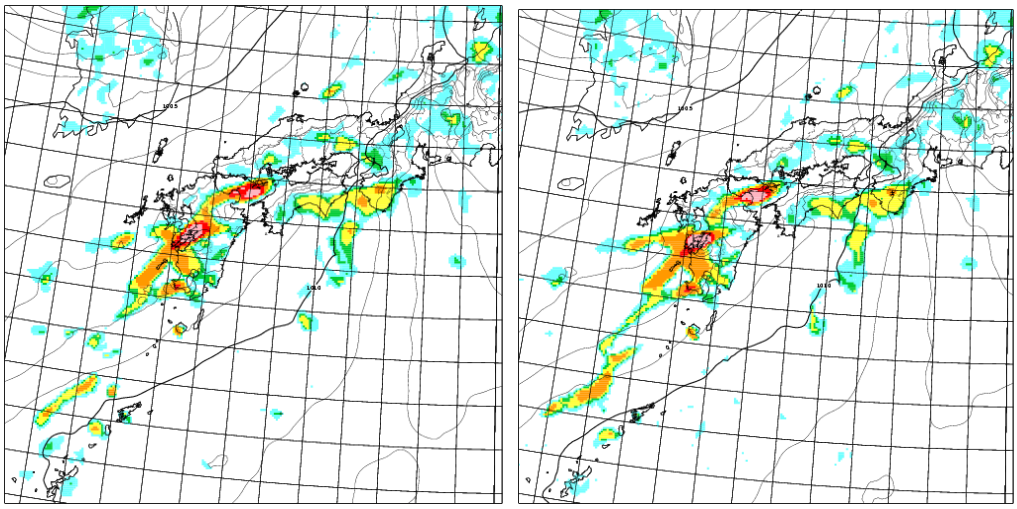

Fig. 2. One hour precipitation at 02 UTC 19 July 2003 predicted by NHM (FT=8hr). **a)** With TMD. **b)** Without TMD.

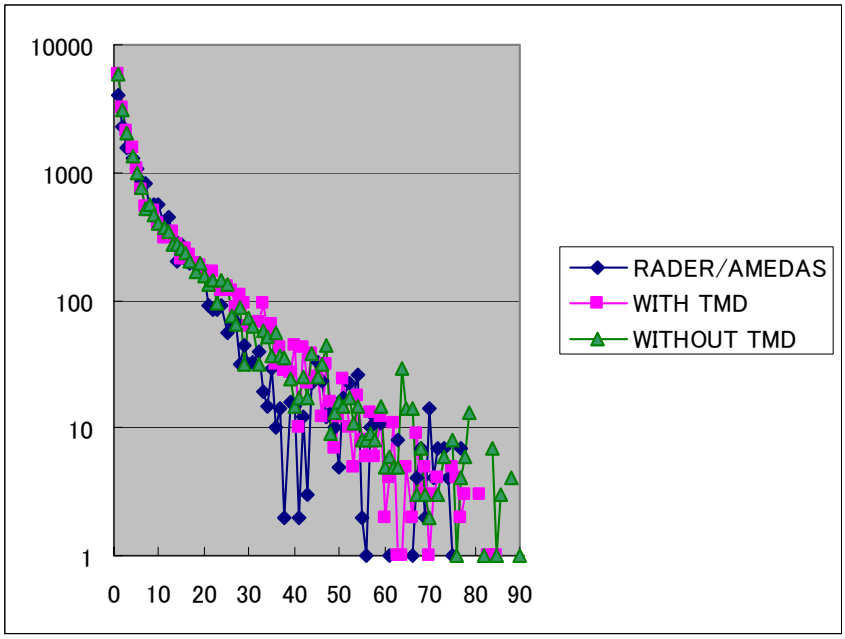

Fig. 3. Histogram of 1 hour precipitation intensity for the model grid of NHM. Horizontal axis is rain intensity (mm/hr), and vertical axis is frequency. The samples are taken from all forecast times of 18 hour forecast starting from 18UTC 18 January 2003.

Operational forecast of the meteorological and turbulence characteristics of the boundary layer

Shnaydman V.A. (State New Jersey University-Rutgers, USA, volf@envsci.rutgers.edu)
Berkovich L. V., Tkacheva Yu.V. (Hydrometeorological Research Center of Russia, berkovich@mecom.ru)

The coupled model for prediction of large and mesoscale atmospheric processes based on the hemispheric forecast model(HFM) and boundary layer model (BLM) described in[1,2] . Let's emphasis the improved two-equation closure scheme is applied in BLM. The operational objective analysis data are the initial for the meteorological variables in the coupled model. By using these data and the one-dimensional version of boundary layer scheme we restored the initial fields of turbulence and meteorological parameters. The implicit time integration scheme with the iterative cycle on each temporal step (approximately 5 iterations) is used in BLM and leap-frog scheme in HFM. The predicted lower and upper boundary conditions for BLM are calculated by HFM. These vertical boundary conditions and the implicit scheme allowed to get the real positive values of turbulent kinetic energy, dissipation rate and avoid the fictive solution that appeared without use of developed method. The turbulence coefficients and friction vertical velocity calculated in boundary model are transferred to HFM. On the pictures the example of the boundary layer parameter 42 hour forecast (noon, 25 July, 2004 in USA) of turbulent energy (m2/s2) increased in 100 times (a), turbulence coefficient (m2/s,c) on the level 100m (b) and friction vertical velocity (mb/ 12 h) on the top of boundary layer (c) is given.

(a)

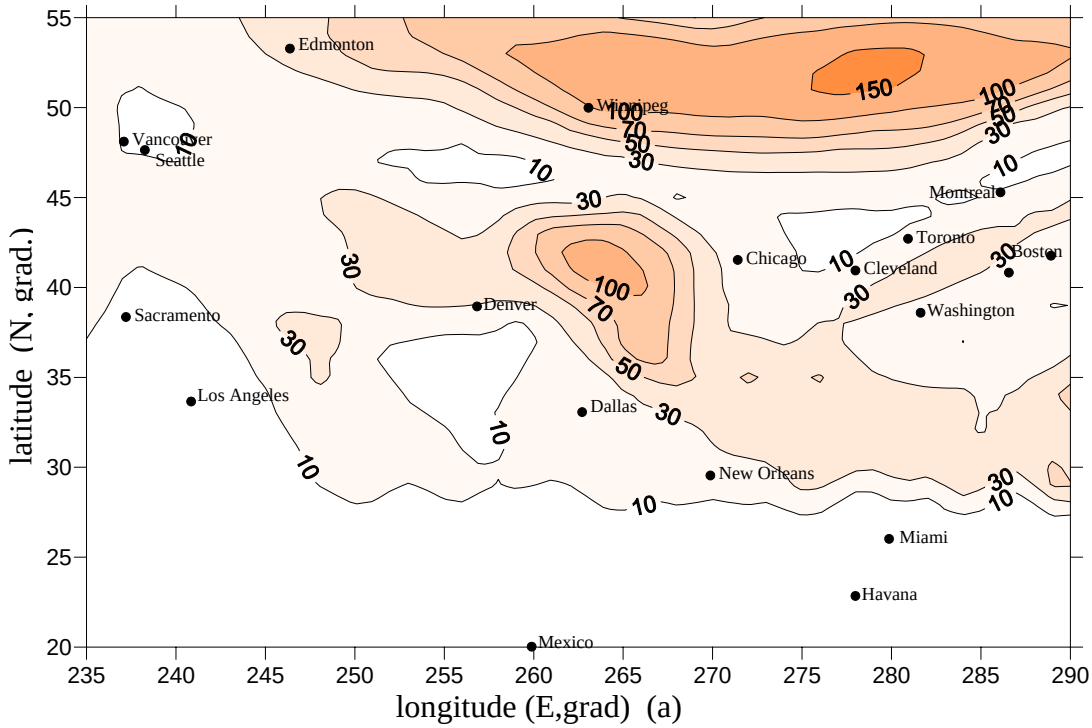

The problem of comparison of the predicted and high resolution actual meteorological variable vertical distribution and turbulence parameters require the special measurements which we didn't have in standard meteorological information. So we used the actual surface and 850 hPa level data on the prediction time as lower and upper boundary conditions and recalculated the boundary layer parameters which we considered as actual values.

Comparison of these values and the predicted ones showed the good agreement of the boundary layer parameters fields. The output of coupled model was compared with the local weather data. The verification of weather forecasts confirmed the high quality of the predicted information .It is a reason to insert the boundary layer model in the coupled model and to use the developed prognostic model for operational practice.

(b)

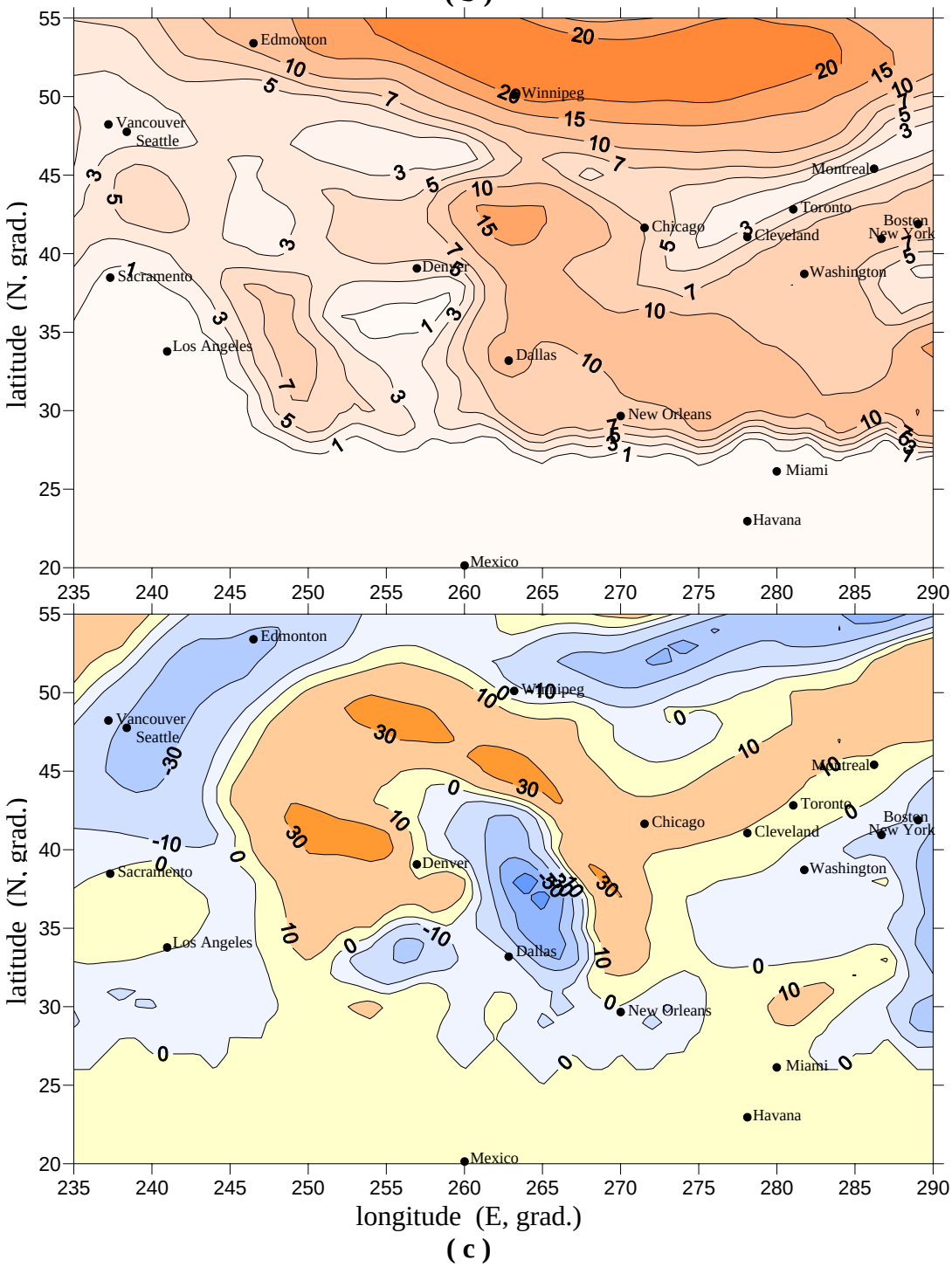

(c)

1.Berkovich L., Tkacheva Yu., The hydrodynamic short-range of local weather forecasting . Research Activity in Atmospheric and Oceanic Modeling, 2003,No 33, 5.1-5.2.

2.Shnaydman V.“ Improved hydrodynamical scheme of the turbulence description “ Research Activity in Atmospheric and Oceanic Modeling, 2004, No 34, 4.29 – 4.30.

Correcting prognostic GRIB data using hi-resolution 3D Lagrangian model.

Roman Solomakhov

MapMakers Group Ltd., Moscow, Russia, E-mail: pdzaccone@gismeteo.com

Multiple cases of serious mismatches between prognostic and observation data, especially in mountainous areas and in regions with poor meteo-stations covering, leaded to the idea of correcting macroscale models' data. These mismatches are caused by 2 main reasons: macro models normally use topography smoothing and thus lower the topography detailing; these models use low-resolution grids, which cannot provide precise calculations. Figure 1 shows you relative error of the 12-hour surface air temperature forecast in Alpine region, figure 2 – around the Yakutsk city. As you can see, these errors can reach up to 20 °C.

To correct prognostic data from macroscale models hi-resolution 3D Lagrangian mesoscale model was developed. This model's input data consist of prognostic GRIB data from big meteorological centers' models, combined (if needed) with surface and aerological observation data. Vertical distribution of wind, temperature and humidity, as well as turbulence characteristics in the lower troposphere are calculated by means of geophysical boundary layer model. [1]

To use terrain data most effectively, model is working in σ-coordinates. While being hi-resolution model using detailed topography data, our model can work on personal computers, i.e. it requires low processor power. Another advantage is its flexible and user-friendly interface, allowing operator not only to specify the model resolution and the vertical levels set according to his needs, but also to set new working territory in several minutes.

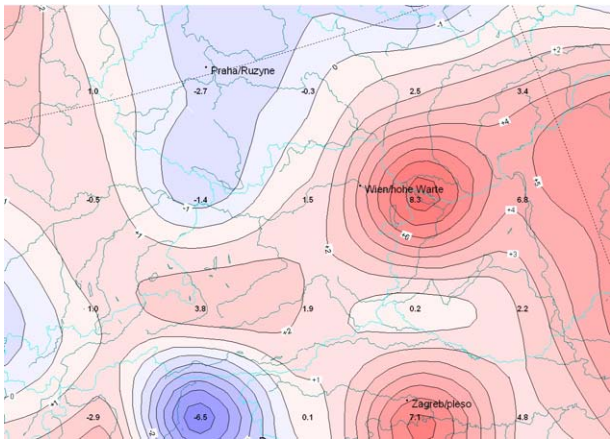

Fig. 1 – Alpine region

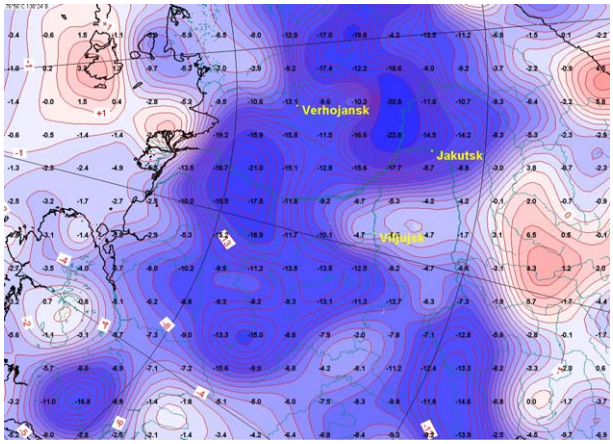

Fig. 2 – around Yakutsk city

References:

1. Berkovich, L.V., Tarnopolskii, A.G., Shnaydman, V.A.: 1997, "A Hydrodynamic Model of the Atmospheric and Oceanic Boundary Layers," Russian Meteorology and Hydrology 7, 30-40
2. Belousov, S.L., Berkovich, L.V., Yusupov Y.I.: 1994, "Short-range Hydrodynamical Weather Forecasting by Means of Automated Workstation Technology," Russian Meteorology and Hydrology 11, 40-52.

A Z-Coordinate Version of the Non-Hydrostatic Model LM

J. Steppeler*, H. W. Bitzer**, Z. Janjic***, U. Schättler*,
P. Prohl*, U. Gjertsen****, J. Parfinievicz*****, U. Damrath*

*DWD juergen.Steppeler@dwd.de
**AW Geophys, ***NCEP, ****met.no, *****IMGW

1. Introduction

A z-coordinate 3-d version LM-Z of the nonhydrostatic model LM (Steppeler et al., 2002a) was created, using the numeric scheme described in Steppeler et. al. 2002b. Mountains are represented by linear splines, as opposed to the step mountain approach of Mesinger et al. (1988) using a representation of the topography by piecewise constant functions. This technique is also known as brick (or Lego) approach and it was shown by Gallus and Klemp (2000) that there are serious problems with this approach in the presence of wind. In test problems it could be shown that the solution does not converge. The technique used in the LM-Z is free from this error.

A number of idealised and real forecast tests have been performed. The large scale features of clouds are captured by LM-Z and LM. Concerning meso scale cloud structures there are substantial differences between the two forecasts. In particular the distinction between cellular and stratiform clouds is more realistic for LM-Z. A case of low stratus over southern Sweden was forecasted as layered cloud with LM-Z and rather broken with LM.

The case shown here is the 30 hr forecast starting from the 28th of March 1997 00 UTC, representing a strong wind situation. The rather interesting differences in the forecast of mesoscale cloud structures result in different precipitation forecasts. Fig 1 shows the observed precipitation sum 29 March 1997 06 to 28 March 1997 06 and the corresponding forecasts of LM and LM-Z. There is a substantial improvement by the LM-Z.

REFERENCES.

Gallus, W., and J. Klemp, 2000: Behavior of flow over step orography. Mon. Wea. Rev., 128, 1153-1164.

Mesinger, F., Z. Janjic, S. Nicovic, D. Gavrilov and D. Deaven, 1988: The step-mountain coordinate: Model description and performance for cases of Alpine lee cyclogenesis and for a case of Appalachian redevelopment. Mon. Wea. Rev. 116, 1493-1518.

Steppeler, J., G. Doms, U. Schättler, H.W. Bitzer, A. Gassmann, U. Damrath and G. Gregoric, 2002a: Meso gamma scale forecasts by nonhydrostatic model LM. Meteor. Atmos. Phys., 82, 75-96.

Steppeler, J., H.W. Bitzer, M. Minotte, L. Bonaventura, 2002b: Nonhydrostatic atmospheric modelling using a z-coordinate representation. Mon. Wea. Rev. 130, 2143-2149.

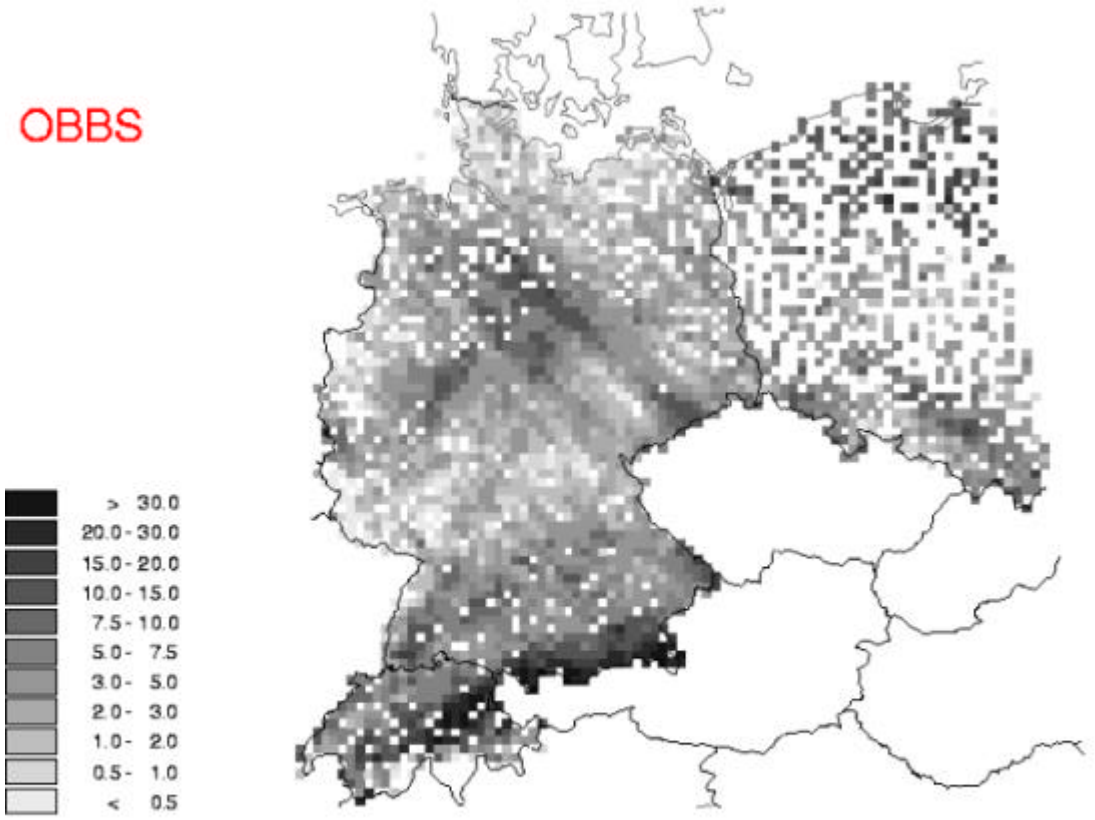

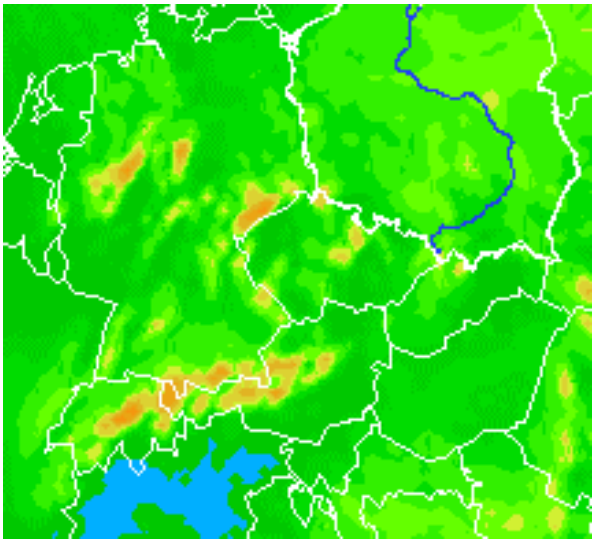

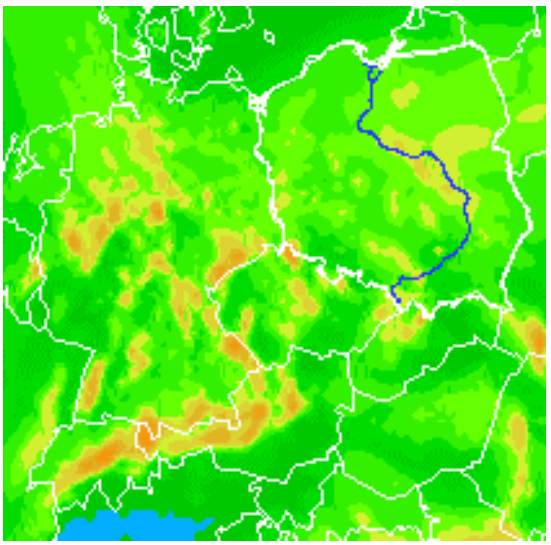

Fig 8 top: The precipitation sum as observed by the climatological network from 28 March 1997 6 UTC to 29 March 1997 6 UTC. Data from Germany, Switzerland and Poland were used; bottom left : As fig. 8 top, but for forecasts of the model LM; bottom right: as fig. 8 left, but for the model LM-Z

Verification in Croatian Meteorological and Hydrological Service

Zoran Vakula, Lovro Kalin, Martina Tudor and Stjepan Ivatek-Šahdan
Meteorological and Hydrological Service, Grič 3, HR-10000 Zagreb, Croatia
vakula@cirus.dhz.hr, kalin@cirus.dhz.hr, tudor@cirus.dhz.hr & ivateks@cirus.dhz.hr

In the Croatian Meteorological and Hydrological Service in year 2004 quite a lot of time was dedicated to verification issues. For more than 3 year "graphical" verification to Croatian SINOP stations for ALADIN/LACE (12 km) and ALADIN/CROATIA (8 km) exist. Example is shown in case study of one extreme event not well forecasted with ALADIN model. From summer 2004 verification against checked hourly data exist, unfortunately with few month delay and just for main stations in Croatia.

Adriatic storm case on 24th March 2004

On 24th March 2004 03 UTC a cyclone stroke a southern part of Croatian coast in the Dubrovnik area. Unfortunately, the movement was forecasted too fast and the depth of this cyclone was severely underestimated. Model outputs have 3 hours interval. On verification figures 3-hourly forecast points are connected with lines and SINOP data are just points.

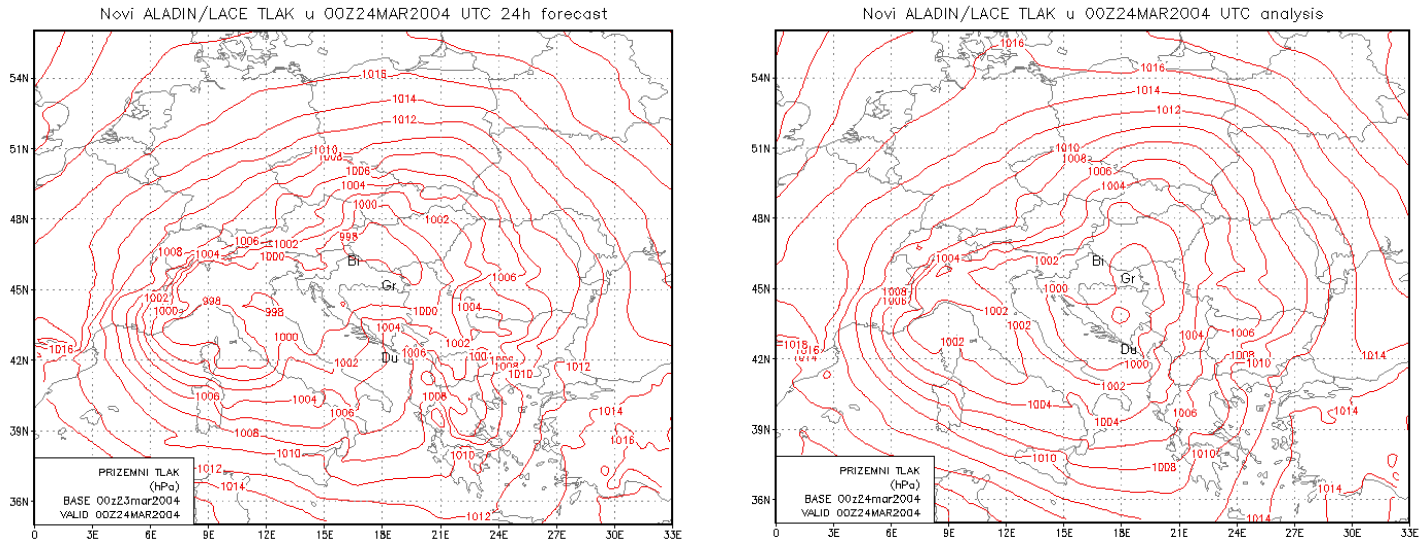

Mean sea level pressure 24 hrs forecast (left) and analysis (left) for 00 UTC 24th March 2004.

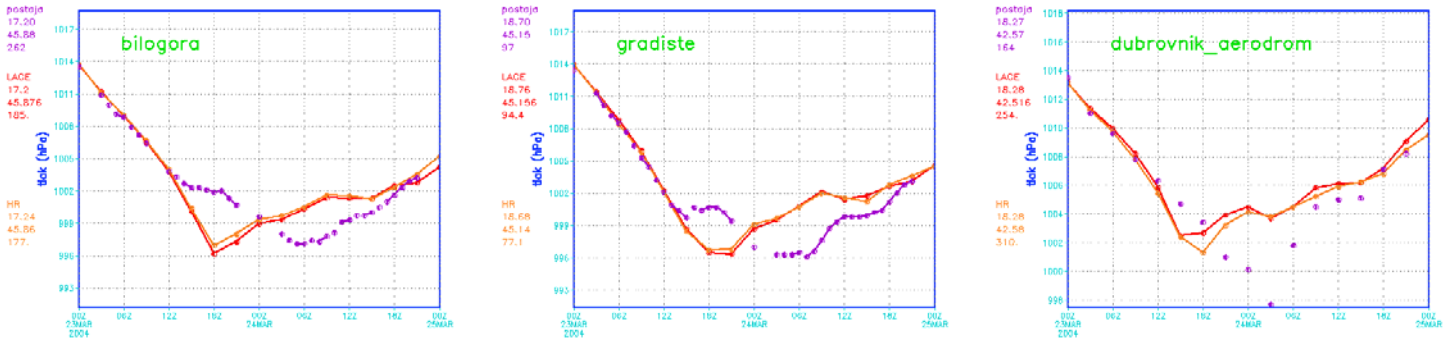

Comparison of the forecasted mean sea level pressure with 12-km (red) and 8-km (orange) with measurements from the SYNOP (violet dots) stations.

New verification products

First new pre-operational verification results of ALADIN forecasts for meteorological stations are shown bellow. At the moment verification of extreme 2 m temperature (daily min & max), precipitation, 10-m wind from surface data are done monthly. As it was before, verification against sounding for station Zagreb Maksimir for ECMWF and ALADIN models are continued. In year 2005 verification against sounding in Zadar is planed.

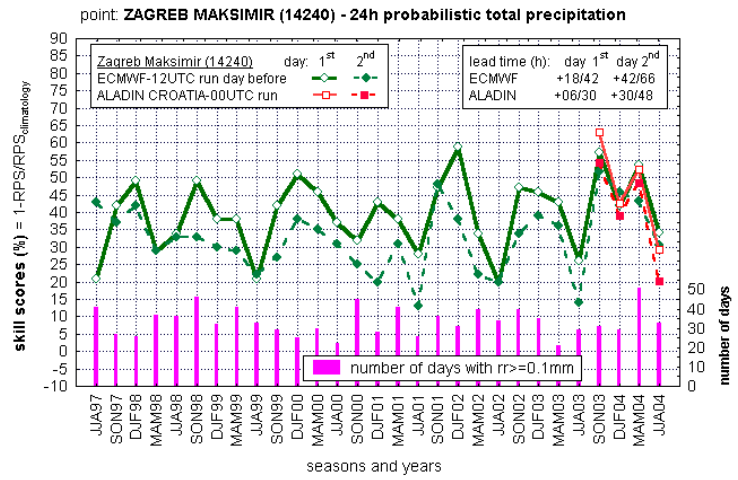

Skill scores for probability of precipitation made of ranked probability scores of quantitative ECMWF and ALADIN CROATIA precipitation forecasts for "1st" and "2nd" day for Zagreb Maksimir (14240), from summer 1997 to summer 2004 (left).

Bias of ALADIN CROATIA precipitation forecast (rain versus no rain) for Zagreb Maksimir (14240), Gospic (14330) and Split Marjan (14445) from September 2003 to March 2004 (bellow left). Mean errors and standard deviation of ALADIN CROATIA wind speed for Split Marjan (14445) for the year 2003 (bellow right).

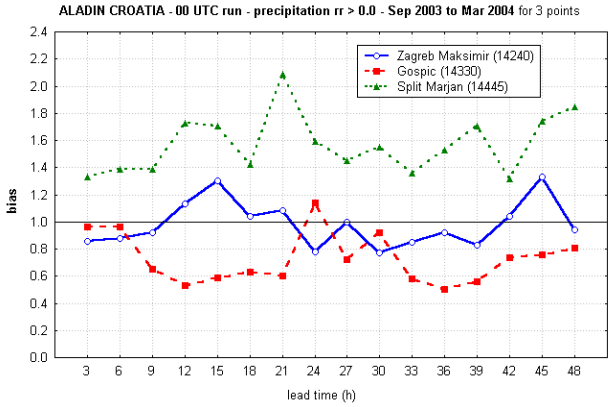

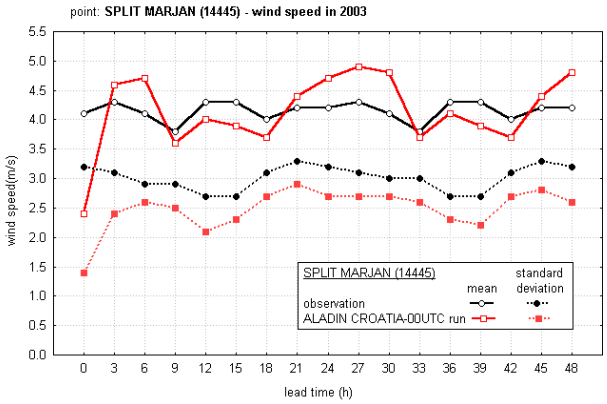

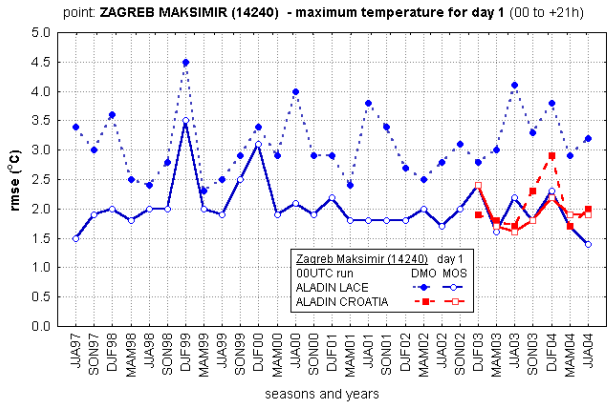

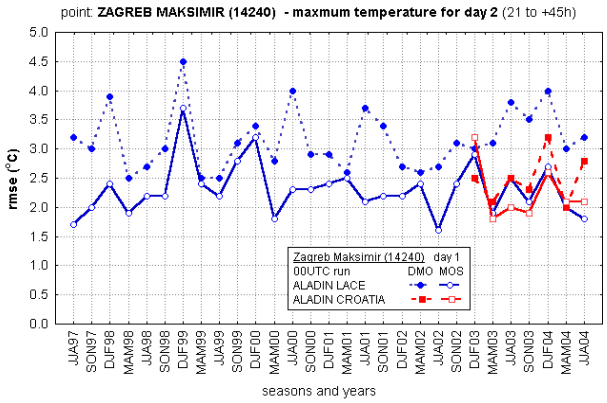

Root-mean-square errors of maximum temperature for day 1 (left) and day 2 (right) forecast of ALADIN LACE (12 km) and CROATIA (8 km) for direct model output and model output statistics, for Zagreb Maksimir, from summer 1997 to summer 2004. MOS are done using regression equations (y=ax+b) which were calculated from historic data for warm (April to September) and cold (October to March) part of the year.

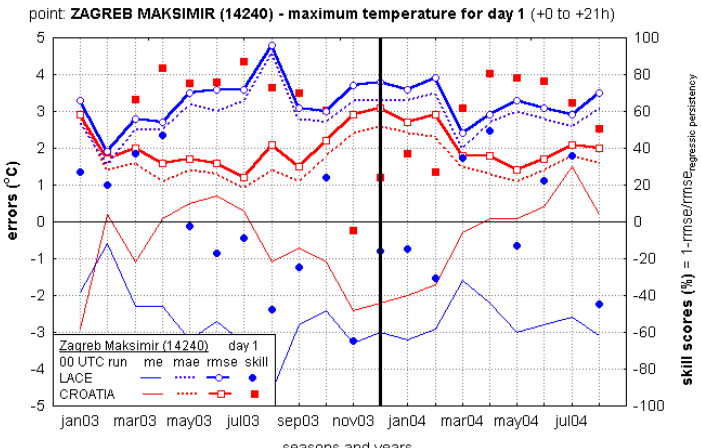

Monthly mean errors, mean absolute errors, root-mean-square errors and skill scores (according root-mean-square error and regression persistency) for day 1 maximum temperature forecast of ALADIN LACE (12 km) and CROATIA (8 km) for direct model output, for Zagreb Maksimir (14240), from January 2003 to August 2004.

For this station forecast of maximum temperature for day 1 and 8 km resolution is better than 12 km resolution. Unfortunately that is not a case for all meteorological stations in Croatia.

Tropical Cyclone Motion and Asymmetry due to Land-sea Friction Contrast

Martin L. M. Wong and Johnny C. L. Chan*
Laboratory for Atmospheric Research, Dept. of Physics and Materials Science
City University of Hong Kong, Hong Kong, China
*Email: Johnny.chan@cityu.edu.hk

Massive destruction of life, property and infrastructure occurs when a tropical cyclone (TC) is near a densely populated region. The movement of a TC near such a region is therefore of more social and economic interests than when it is in the open sea. While significant track deflection can occur when a TC interacts with topography, the possibility of a track deflection due to the different surface fluxes of momentum, heat and moisture have not been addressed. This study investigates such possible vortex motion using the Pennsylvania State University-National Center for Atmospheric Research MM5 model.

Idealized numerical experiments are performed on an *f* plane under no background flow, with an initially symmetric, baroclinic vortex placed 150 km due east of an infinitely long coastline separating land (west of the coast) and sea (east of the coast). The surface temperature is held fixed at 28.5^{o}C over the entire modeling domain. With a specified roughness length of 0.5 m and abundant surface moisture supply (moisture availability 100%) over land, the vortex is found to drift towards land (Fig. 1), with a speed of about 4 km h^{-1}. Using a moisture availability of 5% also results in a similar drift but altering the moisture availability only does not result in a drift (not shown). The difference in surface momentum flux appears to be the cause of the drift.

The difference in surface friction between land and sea could influence the symmetric structure of a TC, and results in vortex drift and asymmetry in rainfall. Two possible mechanisms have been identified. First, boundary-layer convergence is stronger along the coast to the north than to the south of the TC. The convergence pattern above the boundary layer is found to be out-of-phase from that within the boundary layer, and results in the development of larger vorticity to the south than to the north, due to the divergence term in the vorticity equation. The flow within the lower to mid troposphere ($0.9 \geq \sigma \geq 0.55$) indicates the development of an asymmetry consistent with the vorticity development by the divergence term and rotation by the TC circulation (Figs. 2a and 2b). Within the upper troposphere ($0.55 \geq \sigma \geq 0.25$), the asymmetric flow is different (Fig. 2c) and represents a vertical shear of this large-scale asymmetric flow.

The presence of an asymmetric flow represents a 'steering' effect and the vertical shear could generate an asymmetry in vertical motion and rainfall (e.g. Wong and Chan 2004). The direction of the shear vector and the development of a vertical tilt are found to be consistent with the asymmetry in vertical motion and rainfall, which is also found in some previous studies (e.g. Chan and Liang 2003). However, the TC does not move with the steering flow. Investigation of the various terms in the potential vorticity (PV) equation indicates that the vertical advection and diabatic heating terms are also important in determining the PV tendency.

Second, the boundary-layer convergence could force an asymmetry in vertical motion. Additional experiments are performed with the exclusion of moisture and latent heating. The TCs are placed at -150, -100, -50, 0, 50, 100 and 150 km east of the coast. The mass fields (i.e. temperature, pressure) are not allowed to change with time during the 24 h simulation, while the 3-dimensional winds are allowed to adjust to the mass fields and the drag from the surface. When the TC is placed at 50, 100 and 150 km east of the coast, boundary-layer ($1.0 \geq \sigma \geq 0.9$) convergence is much stronger west of the TC, though the averaging area covers the sea only for the TCs placed 100 and 150 km east of the coast (Fig. 3). There is also a small tendency for the asymmetry to rotate slightly anticyclonically as the vortex 'edges closer' to the coast, from 150 km to 50 km (dotted and solid lines respectively). These results are also consistent with the asymmetry in rainfall and vertical motion (not

shown). When the TC is placed at the coast or west of the coast, however, the asymmetry diminishes (not shown).

Acknowledgments. This work is sponsored by the Research Grants Council of the Hong Kong Special Administrative Region, China Grant CityU 100203.

References

Chan, J. C. L., and X. Liang, 2003: Convective asymmetries associated with tropical cyclone landfall. Part I: *f*-plane simulations. *J. Atmos. Sci.,* **60,** 1560-1576.

Wong, M. L. M., and J. C. L. Chan, 2004: Tropical cyclone intensity in vertical wind shear. *J. Atmos. Sci.,* **61,** 1859-1876.

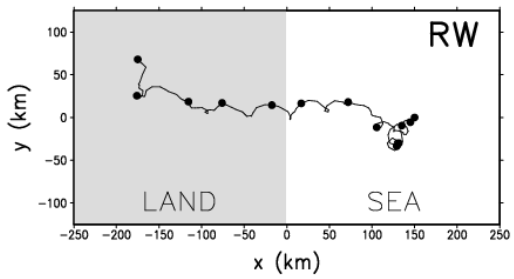

Fig. 1. Track of the TC surface center. Dots denote 12-hourly TC positions. The origin is the location of the domain center.

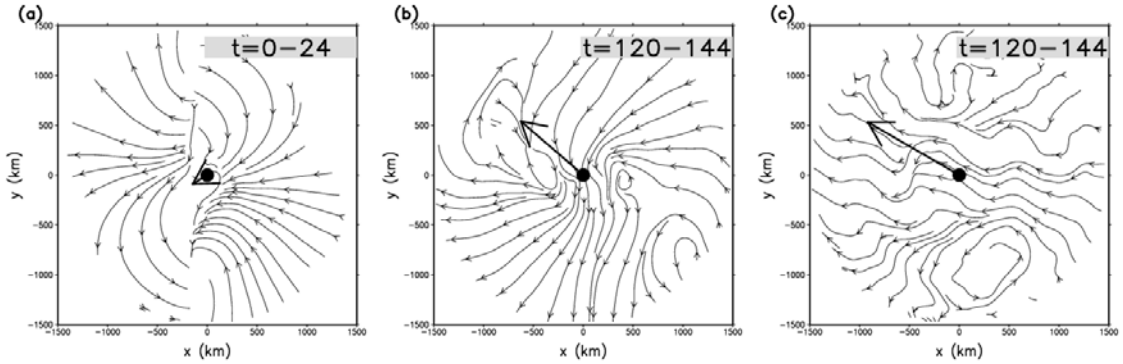

Fig. 2. Time composite of the asymmetric component of the flow for the (a) first day within $0.9 \geq \sigma \geq 0.55$, (b) sixth day within $0.9 \geq \sigma \geq 0.55$ and (c) sixth day within $0.55 \geq \sigma \geq 0.25$. The big arrow indicates the overall movement of the center during that day.

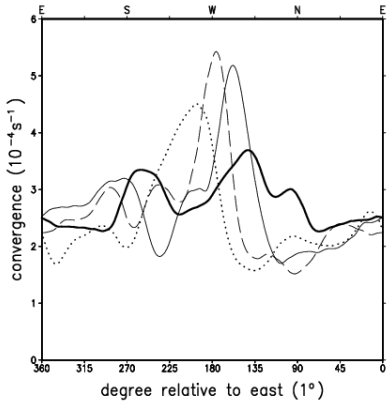

Fig. 3. Boundary-layer ($1.0 \geq \sigma \geq 0.9$) convergence averaged within 100 km at each azimuth for the experiments where the mass fields of the TC are fixed: the TCs are located at 50 (solid), 100 (dashed) and 150 km (dotted) east of the coast. The bold solid line corresponds to the case where the TC is located at the coast.